

**'Multi-model
assessment of ozone
return dates and
recovery**

V. Eyring et al.

Multi-model assessment of stratospheric ozone return dates and ozone recovery in CCMVal-2 models

V. Eyring¹, I. Cionni¹, G. E. Bodeker², A. J. Charlton-Perez³, D. E. Kinnison⁴, J. F. Scinocca⁵, D. W. Waugh⁶, H. Akiyoshi⁷, S. Bekki⁸, M. P. Chipperfield⁹, M. Dameris¹, S. Dhomse⁹, S. M. Frith¹⁰, H. Garny¹, A. Gettelman⁴, A. Kubin¹¹, U. Langematz¹¹, E. Mancini¹², M. Marchand⁸, T. Nakamura⁷, L. D. Oman^{13,6}, S. Pawson¹³, G. Pitari¹², D. A. Plummer⁵, E. Rozanov^{14,15}, T. G. Shepherd¹⁶, K. Shibata¹⁷, W. Tian⁹, P. Braesicke¹⁸, S. C. Hardiman¹⁹, J. F. Lamarque⁴, O. Morgenstern^{18,20}, J. A. Pyle¹⁸, D. Smale²⁰, and Y. Yamashita^{21,7}

¹Deutsches Zentrum für Luft- und Raumfahrt, Institut für Physik der Atmosphäre, Oberpfaffenhofen, Germany

²Bodeker Scientific, Alexandra, New Zealand

³University of Reading, Department of Meteorology, Reading, UK

⁴National Center for Atmospheric Research, Boulder, CO, USA

⁵Environment Canada, Victoria, BC, Canada

Title Page

Abstract

Introduction

Conclusions

References

Tables

Figures

⏪

⏩

◀

▶

Back

Close

Full Screen / Esc

Printer-friendly Version

Interactive Discussion

**'Multi-model
assessment of ozone
return dates and
recovery**

V. Eyring et al.

Title Page

Abstract

Introduction

Conclusions

References

Tables

Figures

⏪

⏩

◀

▶

Back

Close

Full Screen / Esc

Printer-friendly Version

Interactive Discussion



⁶ Johns Hopkins University, Department of Earth and Planetary Sciences, Baltimore, Maryland, USA

⁷ National Institute for Environmental Studies, Tsukuba, Japan

⁸ Service d'Aéronomie, Institut Pierre-Simone Laplace, Paris, France

⁹ Institute for Climate and Atmospheric Science, University of Leeds, UK

¹⁰ Science Systems and Applications, Inc., Lanham MD 20706, USA

¹¹ Freie Universität Berlin, Institut für Meteorologie, Berlin, Germany

¹² Università L'Aquila, Dipartimento di Fisica, L'Aquila, Italy

¹³ NASA Goddard Space Flight Center, Greenbelt, Maryland, USA

¹⁴ Physikalisch-Meteorologisches Observatorium Davos/World Radiation Center, Davos, Switzerland

¹⁵ Institute for Atmospheric and Climate Science ETH, Zurich, Switzerland

¹⁶ University of Toronto, Department of Physics, Canada

¹⁷ Meteorological Research Institute, Tsukuba, Japan

¹⁸ University of Cambridge, Department of Chemistry, Cambridge, UK

¹⁹ Met Office, Exeter, UK

²⁰ National Institute of Water and Atmospheric Research, Lauder, New Zealand

²¹ Center for Climate System Research, University of Tokyo, Japan

Received: 24 March 2010 – Accepted: 27 April 2010 – Published: 3 May 2010

Correspondence to: V. Eyring (veronika.eyring@dlr.de)

Published by Copernicus Publications on behalf of the European Geosciences Union.

Abstract

Projections of stratospheric ozone from a suite of chemistry-climate models (CCMs) have been analyzed. In addition to a reference simulation where anthropogenic halogenated ozone depleting substances (ODSs) and greenhouse gases (GHGs) vary with time, sensitivity simulations with either ODSs or GHGs concentrations fixed at 1960 levels were performed to disaggregate the drivers of projected ozone changes. These simulations were also used to assess the two distinct milestones of ozone returning to historical values (ozone return dates) and ozone no longer being influenced by ODSs (full ozone recovery). These two milestones are different. The date of ozone returning to historical values does not indicate complete recovery from ODSs in most cases, because GHG induced changes accelerate or decelerate ozone changes in many regions. In the upper stratosphere where GHG induced stratospheric cooling increases ozone, full ozone recovery has not likely occurred by 2100 while ozone returns to its 1980 or even 1960 levels well before (~2025 and 2040, respectively). In contrast, in the tropical lower stratosphere ozone decreases continuously from 1960 to 2100 due to projected increases in tropical upwelling, while by around 2040 it is already very likely that full recovery from the effects of ODSs has occurred, although ODS concentrations are still elevated by this date. In the lower midlatitude stratosphere the evolution differs from that in the tropics, and rather than a steady decrease of ozone, first a decrease of ozone is simulated between 1960 and 2000, which is then followed by a steady increase throughout the 21st century. Ozone in the lower stratosphere midlatitudes returns to its 1980 levels ~2045 in the NH and ~2055 in the SH, and full ozone recovery is likely reached by 2100 in both hemispheres. Overall, in all regions except the tropical lower stratosphere, full ozone recovery from ODSs occurs significantly later than the return of total column ozone to its 1980 level. The latest return of total column ozone is projected to occur over Antarctica (~2050–2060) whereas it is not likely that full ozone recovery is reached by the end of the 21st century in this region. Arctic total column ozone is projected to return to 1980 levels well before Cl_y does so (~2020–2030) and

'Multi-model assessment of ozone return dates and recovery

V. Eyring et al.

Title Page

Abstract

Introduction

Conclusions

References

Tables

Figures



Back

Close

Full Screen / Esc

Printer-friendly Version

Interactive Discussion



while it is likely that full recovery of ozone from the effects of ODSs has occurred by ~2035, at no time before 2100 is it very likely that full recovery has occurred. In contrast to the Antarctic, by 2100 Arctic total column ozone is projected to be above 1960 levels, but not in the fixed GHG simulation, indicating that climate change plays a significant role.

1 Introduction

Stratospheric ozone has been depleted by anthropogenic emissions of halogenated species over the last decades of the 20th century. In particular, emissions of anthropogenic halogenated Ozone Depletion Substances (ODSs) whose production is controlled under the Montreal Protocol and its Amendments and Adjustments have increased stratospheric chlorine and bromine concentrations as measured by an increase in equivalent stratospheric chlorine (ESC) and have dominated ozone loss in the recent past (Shepherd and Jonsson, 2008). Observations show that tropospheric halogen loading peaked around 1993 and is now decreasing (Montzka et al., 2003; WMO, 2007), reflecting the controls on ODS production by the Montreal Protocol. This slow decline is expected to continue through the 21st century and ozone is expected to recover from the effect of ODSs as their concentrations reach their unperturbed values (Eyring et al., 2007; WMO, 2007). Atmospheric concentrations of long-lived greenhouse gases (GHGs) have also increased and are expected to increase further in the future (IPCC, 2000) with consequences for the ozone layer. As stratospheric ODS concentrations slowly decline, effects of other processes such as GHG induced changes in stratospheric temperatures, chemistry, circulation and transport are likely to play a more important role in the evolution of ozone through the 21st century (Randeniya et al., 2002; Rosenfield et al., 2002; Haigh and Pyle, 1982; Chipperfield and Feng, 2003; Portmann and Solomon, 2007; Garcia et al., 2007; Ravishankara et al., 2009, Butchart et al., 2006, 2010; Oman et al., 2010a, b). The importance of these factors varies with region and time and thus the evolution of stratospheric ozone in the 21st century also

'Multi-model assessment of ozone return dates and recovery

V. Eyring et al.

Title Page

Abstract

Introduction

Conclusions

References

Tables

Figures

⏪

⏩

◀

▶

Back

Close

Full Screen / Esc

Printer-friendly Version

Interactive Discussion



varies with region.

To project the future evolution of stratospheric ozone and attribute its behavior to different forcings, Chemistry-Climate Models (CCMs) are widely used (e.g. Eyring et al., 2007; WMO, 2007). CCMs are three-dimensional atmospheric circulation models with fully coupled stratospheric chemistry, i.e. where chemical reactions drive changes in the atmospheric composition of trace gases which in turn change the atmospheric radiative balance and hence dynamics. The pool of CCMs, and the number of simulations performed, has significantly deepened over the past four years. In particular simulations from 15 CCMs that participated in the second round of coordinated model inter-comparison organized by the Chemistry-Climate Model Validation (CCMVal) Activity (Eyring et al., 2005) (hereafter referred to as CCMVal-2) have been used to predict the evolution of stratospheric ozone through the 21st century (Austin et al., 2010). These CCMs have also been extensively evaluated as part of the Stratospheric Processes And their Role in Climate (SPARC) CCMVal Report (SPARC CCMVal, 2010). Following the completion of the SPARC CCMVal Report, sensitivity simulations defined by Eyring et al. (2008) with either ODSs or GHGs fixed at 1960 levels have been completed by a subset of 10 CCMs and are analyzed here in addition to the future reference simulations with varying ODSs and GHGs to quantitatively disaggregate the drivers of the projected ozone changes and to study important milestones along the road of full ozone recovery.

The focus of the analysis is on the assessment of the two distinct milestones of ozone returning to historical values (ozone return dates) and ozone being no longer influenced by ODSs (full ozone recovery), following the definitions of WMO (2007). It is important to note that the date of ozone returning to historical values (e.g. mean 1960 or 1980 values) does not indicate complete recovery from ODSs in most cases, because GHG induced changes accelerate or decelerate ozone changes in many regions. Full ozone recovery has so far only been studied with a single model (Waugh et al., 2009), and it is important to test these findings in a multi-model framework. In addition, the “no greenhouse-gas induced climate change” simulations with fixed GHGs were performed

**'Multi-model
assessment of ozone
return dates and
recovery**

V. Eyring et al.

Title Page

Abstract

Introduction

Conclusions

References

Tables

Figures

⏪

⏩

◀

▶

Back

Close

Full Screen / Esc

Printer-friendly Version

Interactive Discussion



by single models to address the nonlinearity of ozone depletion/recovery and climate change (Garcia and Randel, 2008; Chapter 5 of WMO, 2007; Akiyoshi et al., 2010; McLandress et al., 2010).

The models and simulations are described in Sect. 2 and the method to generate the multi-model time series and associated uncertainties is described in Sect. 3. Section 4 uses the two sensitivity simulations with either ODSs or GHGs fixed at 1960 levels to attribute changes in the long-term ozone evolution to changes in ODSs and GHGs. Ozone return dates and the timing of full recovery of ozone from the effects of ODSs are discussed in Sect. 5. Section 6 closes with discussion and conclusions.

2 Models and model simulations

In the SPARC CCMVal Report on the evaluation of CCMs (SPARC CCMVal, 2010), 15 CCMs contributed a future reference simulation (REF) to the CCMVal-2 activity and were used to project ozone through the 21st century. In this study we have added a future reference simulation from the EMAC-FUB model. As a result, some of the results derived from the multi-model mean of the 16 reference simulations shown here differ slightly from those presented in SPARC CCMVal (2010) and Austin et al. (2010). 10 CCM groups also performed additional simulations with GHGs or ODSs fixed at 1960 values which are used here to attribute changes in ozone to these two primary drivers and to assess the milestone of ozone recovery. The participating CCMs are listed in Table 1 and are described in detail in the cited literature as well as in Morgenstern et al. (2010) and Chapter 2 of SPARC CCMVal (2010). It should be noted that only 1 of the 16 CCMs (CMAM) is coupled to an ocean in CCMVal-2, whereas in all other CCMs sea surface temperatures (SSTs) and sea ice concentrations (SICs) are prescribed. The CCMs have been extensively evaluated as part of the SPARC CCMVal Report. This comprehensive process-oriented validation has improved understanding of the strengths and weaknesses of CCMs and has been used to understand some of the source of the spread in model projections.

'Multi-model assessment of ozone return dates and recovery

V. Eyring et al.

Title Page

Abstract

Introduction

Conclusions

References

Tables

Figures



Back

Close

Full Screen / Esc

Printer-friendly Version

Interactive Discussion



In total, 16 CCMs provided a reference simulation, 9 contributed a fixed ODS simulation (*fODS*), and 8 a fixed GHG simulation (*fGHG*). The model simulation design by each model group varied slightly. All simulations are continuous simulations from 1960 to 2100, except that REF and *fGHG* by E39CA ended in 2050, *fGHG* by EMAC-FUB ended in 2050, REF by UМУKCA-METO ended in 2083, and the simulations by GEOSCCM combine a past (1960 to 2000) simulation forced by observed SSTs with a future (2000-2100) simulation so are not continuous. Specifics of the sensitivity simulations for the individual CCMs are summarized in Table 2, and are further detailed in Eyring et al. (2008).

- *REF* is the so-called reference simulation and is a self consistent transient simulation from 1960 to 2100. In this simulation the surface time series of halocarbons are based on the adjusted A1 scenario from WMO (2007). The adjusted A1 halogen scenario includes the earlier phase out of hydrochlorofluorocarbons (HCFCs) that was agreed to by the Parties to the Montreal Protocol in 2007. The long-lived GHG surface concentrations are taken from the SRES (Special Report on Emission Scenarios) GHG scenario A1b (IPCC, 2000). Except in one model (CMAM), SSTs and SICs are prescribed from coupled ocean model simulations, either from simulations with the ocean coupled to the underlying general circulation model, or from coupled ocean-atmosphere models used in IPCC AR-4 simulations under the same GHG scenario. The reference simulation is identical to the SCN-B2d simulation defined in Eyring et al. (2008) for the models that considered forced natural variability (solar cycle and assimilated a quasi-biennial oscillation (QBO)) also in the future (E39CA and EMAC-FUB) while it is identical to the REF-B2 simulation for the models that performed the reference simulation without forced natural variability (all other CCMs).
- *fODS* is a transient simulation from 1960 to 2100 similar to REF, but with ODSs fixed at 1960 levels throughout the simulation. The simulation is designed to address the question of what are the effects of halogens on stratospheric ozone

'Multi-model assessment of ozone return dates and recovery

V. Eyring et al.

[Title Page](#)[Abstract](#)[Introduction](#)[Conclusions](#)[References](#)[Tables](#)[Figures](#)[⏪](#)[⏩](#)[◀](#)[▶](#)[Back](#)[Close](#)[Full Screen / Esc](#)[Printer-friendly Version](#)[Interactive Discussion](#)

**'Multi-model
assessment of ozone
return dates and
recovery**

V. Eyring et al.

Title Page

Abstract

Introduction

Conclusions

References

Tables

Figures



Back

Close

Full Screen / Esc

Printer-friendly Version

Interactive Discussion



and climate in the presence of climate change. By comparing fODS with REF, the impact of halogens can be identified and, within uncertainty associated with unforced inter-annual variability in ozone, it can be assessed at what point in the future the halogen impact on ozone is undetectable, i.e. when full recovery of ozone from the effects of ODSs occurs (WMO, 2007). The fODS simulation also permits an examination of how equivalent stratospheric chlorine (ESC) is affected by climate change alone. This sensitivity simulation is identical to the SCN-B2b simulation defined in Eyring et al. (2008). It should be noted that most models fixed halogens in the radiation and used GHGs and SSTs/SICs from REF (see Table 2). This introduces an inconsistency since with the absence of halogen increases in the radiation less near-surface warming in this experiment should be expected so that the SSTs/SICs from the REF simulations could be too warm.

- *fGHG* is a transient simulation from 1960 to 2100, similar to REF, but with GHGs fixed at 1960 levels throughout the simulation. To be consistent with the GHG evolution, SSTs and SICs are prescribed with the 1955-1964 average of the values used in REF. This was done in all but one such model simulation (SOCOL). In the Socol *fGHG* simulation, the same time varying SSTs/SICs as in REF were used which provides the basis for a qualitative evaluation of the effect of SSTs alone on stratospheric ozone under fixed GHG loading (not part of this study), but introduces a significant inconsistency with the GHG evolution. Whether or not the chemical effects of CH₄ and N₂O on ozone were also fixed at 1960 levels varied between the different modeling groups (see Table 2). The intention of the *fGHG* simulation was that the ODSs (in particular the CFCs) should also not contribute to radiative forcing. However, in a number of CCMs it was only the radiative forcing for CO₂, CH₄ and N₂O that was held constant at 1960 values. The simulation is designed to address the issue of the linear additivity of the effects of GHGs and ODSs on ozone through the 21st century. By comparing the sum of *fGHG* and fODS (each relative to the 1960 baseline) with REF, the linear additivity of the responses can be assessed. This sensitivity simulation is identical to the SCN-B2c

simulation defined in Eyring et al. (2008).

3 Analysis method for multi-model time series

The same time series additive model (TSAM) as used in Chapter 9 of SPARC CCMVal (2010) and described further in Scinocca et al. (2010) is used here to calculate multi-model time series and their confidence and prediction uncertainties. Anomaly time series relative to a particular reference year (here 1960 and 1980) are calculated for ozone and other species for each model. The values of the reference year for each model which were used to calculate the anomaly time series is obtained from a smooth fit to the time series obtained from the TSAM nonparametric additive model. This smooth fit is referred to as the individual model trend (IMT) estimate. The average of the IMT estimates over all models results in a multi-model trend (MMT) estimate. Here the term 'trend' does not denote the result of a linear regression analysis but rather refers to a smooth trajectory passing through the data representing the "signal" resulting from forced changes and leaving "noise" as a residual resulting from internal unforced climate variability. Both the IMT and MMT estimates pass through zero at the specified reference year. Two types of uncertainty intervals are constructed for the MMT estimate. The first is the point-wise 95% confidence interval. This interval has a 95% chance of overlapping the true trend representing the local uncertainty in the trend at each year. The second interval is the 95% prediction interval which, by construction, is larger than the confidence interval. This interval is a combination of uncertainty in the trend estimate and uncertainty due to natural inter-annual variability about the trend and gives a sense of where an ozone value for a given year might reasonably lie. Some CCMs submitted more than one reference simulation (CMAM, MRI, SOCOL, ULAQ, and WACCM). In such cases the nonparametric regression is applied to the raw time series from all ensemble members to calculate a single IMT which then contributes to the multi-model mean.

To illustrate the TSAM technique, the individual IMT and MMT estimates of the global

'Multi-model assessment of ozone return dates and recovery

V. Eyring et al.

Title Page

Abstract

Introduction

Conclusions

References

Tables

Figures

⏪

⏩

◀

▶

Back

Close

Full Screen / Esc

Printer-friendly Version

Interactive Discussion



**'Multi-model
assessment of ozone
return dates and
recovery**

V. Eyring et al.

Title Page

Abstract

Introduction

Conclusions

References

Tables

Figures

⏪

⏩

◀

▶

Back

Close

Full Screen / Esc

Printer-friendly Version

Interactive Discussion



total column ozone anomaly time series for the 16 reference simulations (REF) are shown in Fig. 1. While the 1980 return date (red vertical lines) is the same in both panels, the uncertainty (blue vertical lines) in return dates derived from the 1960 baseline adjusted column ozone anomalies is slightly larger (by up to 3 years). A summary of the dates when total column ozone returns to its 1980 values, calculated from the two different time series, is given in Table 3. For consistency with the analysis presented in WMO (2007), 1980 ozone return dates in the reference simulations (Sect. 5) were calculated from the 1980-baseline adjusted time series. However, when using the fixed halogen and fixed GHG simulations to disentangle the effects of changes in climate and ODSs on ozone (Sect. 4) and to calculate dates of full recovery of ozone from the effects of ODSs (Sect. 5), the 1960-baseline adjusted time series are used since the halogens and GHGs are fixed at 1960 values and thus the ozone time series are already quite different from the REF simulations by 1980.

4 Long-term ozone evolution and attribution to different forcings

To attribute long-term changes in ozone to GHGs and ODSs, in this section the evolution of ozone in the reference simulations (REF) is compared to the fixed ODS (fODS) and to the fixed GHG (fGHG) simulations. The ozone evolution from 1960 to 2100 is assessed in the context of the 1960 baseline-adjusted ozone, temperature, transformed Eulerian mean vertical velocity (w^*), and total column ozone time series (Figs. 2–5 and 7–9) and additionally ozone and total column ozone are plotted against equivalent stratospheric chlorine (ESC, Figs. 6 to 10) using the absolute values rather than anomalies. In the 1960-baseline adjusted total column ozone, 1960 is used as the reference date from which the individual model trend (IMT) anomalies are calculated in the reference and sensitivity simulations.

4.1 Tropical ozone

In the tropical upper stratosphere, all REF simulations indicate decreasing annual mean ozone between 1960 and 2000 followed by a steady increase until the end of the 21st century, while in the tropical lower stratosphere continuous ozone decreases from 1960 to 2100 are simulated in all models (Fig. 2a and b; see also Chapter 9 of SPARC CCMVal (2010), Austin et al. (2010) and Oman et al. (2010b)). The absolute values for each model in various regions and altitudes are shown in Figs. SM1 to SM25 in the supplementary online material.

The elevated ozone in the tropical upper stratosphere at 5 hPa after 2000 (Fig. 2a) results from a continuous cooling (Fig. 3a) caused by increasing CO₂, which slows gas-phase ozone loss cycles (e.g., Haigh and Pyle, 1982; Rosenfield et al., 2002; Jonsson et al., 2004). The cooling is similar in the fODS simulations (compare solid and long dashed traces in Fig. 3a for the individual models and the MMT), whereas in the fGHG simulations temperatures stay nearly constant over the simulated period because GHGs are fixed at 1960 levels and SSTs/SICs are forced to represent 1960 conditions (Fig. 4a). Consistently, the fGHG simulations show a smaller increase in tropical upper stratospheric ozone from 2000 to 2100 than the REF simulations (Fig. 5a), confirming that the CCMs are able to simulate the mechanism invoked above. In contrast, in the fODS simulation, a steady increase in tropical upper stratospheric ozone is simulated over the entire 1960 to 2100 period (Fig. 2a). At the end of the 21st century, upper stratospheric ozone in all the fGHG simulations is significantly lower than in the REF simulations (Fig. 5a), which in turn is only slightly smaller than the fODS simulations (Fig. 2a).

The data plotted in Figs. 1 to 5 can be presented in an alternative format by plotting ozone as a function of ESC rather than time. This provides a different view on how past and future ozone changes respond to the primary driver of interest i.e. changes in stratospheric halogen loading. An attribution of ozone changes in the tropical upper stratosphere to changes in ODSs and GHGs is displayed in

ACPD

10, 11659–11710, 2010

'Multi-model assessment of ozone return dates and recovery

V. Eyring et al.

Title Page

Abstract

Introduction

Conclusions

References

Tables

Figures

⏪

⏩

◀

▶

Back

Close

Full Screen / Esc

Printer-friendly Version

Interactive Discussion

5 this alternative format in Fig. 6a. The multi-model mean shown in the figure is calculated from the CCSRNIES, MRI, SOCOL and WACCM models. CMAM was excluded from this multi-model mean since the CMAM fGHG simulation included the transient chemical effects of CH₄ and N₂O which cause the 2000 to 2100 fGHG trace to lie below the 1960 to 2000 trace in contrast to the other models used in the multi-model mean which show close concurrence between the 1960–2000 and 2000–2100 segments of the fGHG plot (see Figs. SM1 to SM5 in supplementary online material, <http://www.atmos-chem-phys-discuss.net/10/11659/2010/acpd-10-11659-2010-supplement.pdf>). Furthermore, ULAQ was excluded from this multi-model mean since it too showed behavior quite different to the other four models, including disagreement between the 1960–2000 and 2000–2100 segments in the fGHG simulation (see figures in the supplementary online material). The multi-model mean REF simulation in Fig. 6a shows that ozone decreases from 1960 to 2000 in the upper stratosphere in response to increasing ESC. However, as ESC decreases from 2000 to 2100 ozone does not simply retrace the 1960–2000 path but shows systematically elevated ozone through the 21st century such that ozone returns to 1980 values in the late 2020s well before ESC returns to its 1980 value in the mid-2050s. As discussed above, the elevated ozone through the 21st century results from CO₂ induced stratospheric cooling, shown by the red to blue transition from 1960 to 2100 in the REF trace in Fig. 6a. The fixed ODS simulation shows ozone in the upper stratosphere slowly increasing with time under the influence of increasing CO₂ and resultant stratospheric cooling. In contrast to the REF simulation, the fixed GHG simulation shows that the response of ozone to ESC through the 21st century is almost identical to that through the 20th century. In this simulation, because GHGs are fixed, temperatures show almost no trend from 1960 to 2100 (see also Fig. 4a). To test whether the perturbations to ozone from ODS and GHG changes are independent, the ozone changes due to the combined effect of ODSs and GHGs changes in REF are compared to the sum of the ozone changes due to only the effect of ODSs (fGHG) and due to only effects of GHGs (fODS). The comparison is then used to test whether these two effects on ozone are

**'Multi-model
assessment of ozone
return dates and
recovery**V. Eyring et al.

Title Page

Abstract

Introduction

Conclusions

References

Tables

Figures



Back

Close

Full Screen / Esc

Printer-friendly Version

Interactive Discussion



linearly additive i.e. whether the effect of ODSs (or GHGs) on ozone depends on GHG (or ODS) levels. The close agreement between the REF and grey traces in Fig. 6a indicates that the system is close to being linearly additive. The system deviates most from linear additivity in 2000 when the ozone depletion is largest. The causes for such deviations in linear additivity are not yet known.

In the tropical lower stratosphere, a robust feature simulated by all CCMs is that ozone in the REF simulations shows steadily declining values from 1960 to 2100 and ozone never returns to its 1980 value (Fig. 2b). The primary mechanism causing this trend is the increase in tropical upwelling through the 21st century, which is also a robust result in CCM simulations (see Fig. 7 as well as Butchart et al. (2006, 2010); Oman et al. (2010b); Chapter 4 of SPARC CCMVal (2010)). A future increase in upwelling in the tropics brings ozone poor air from the troposphere into the tropical lower stratosphere, decreasing ozone in this altitude region. The increase in tropical upwelling in fODS is similar to that in REF in all models, confirming that changing halogens do not contribute to this trend which is caused by climate change and in particular climate-change induced SST changes. This is also evidenced by the increase in upwelling in the SOCOL fGHG simulation in which GHGs were fixed but SSTs evolved as in REF (compare dotted and dashed lines to solid lines in Fig. 7), confirming previous findings (Fomichev et al., 2007; Deckert and Dameris, 2008a, b; Oman et al., 2009). In all other CCMs there is no increase in tropical upwelling in the fGHG simulation. Correspondingly, in all but two models (SOCOL and ULAQ), ozone in the tropical lower stratosphere (50 hPa) fGHG simulations stays nearly constant throughout the 21st century (Fig. 5b), whereas ozone in the fODS is very similar to REF (see black dotted line in Fig. 2b), indicating that this region is mainly controlled by changes in climate rather than ODSs. In the tropical lower stratosphere, ULAQ has a higher sensitivity of ozone to halogens than all other models (see also Fig. 4 of Oman et al., 2010b) which could explain why in this simulation the suppressed tropical ozone, unlike in all other models, is mainly determined by halogen changes until 2030. This is concluded from the fact that fGHG in ULAQ is nearly identical to REF until 2030 (Fig. 5b). Only after 2030

**'Multi-model
assessment of ozone
return dates and
recovery**V. Eyring et al.

[Title Page](#)[Abstract](#)[Introduction](#)[Conclusions](#)[References](#)[Tables](#)[Figures](#)[Back](#)[Close](#)[Full Screen / Esc](#)[Printer-friendly Version](#)[Interactive Discussion](#)

does climate change dominate halogen sensitivity in ULAQ. One reason for this could be the coarse horizontal resolution in ULAQ or that the model includes an explicit code for NAT and ice particle formation, growth and transport which can form not only in the winter polar regions but also in the tropical UTLS. In addition, ULAQ includes a parameterization for upper tropospheric cirrus ice particles (Kärcher and Lohmann, 2002). Ozone in the lower stratosphere and total column ozone in the 2nd half of the 21st century in the REF simulation of SOCOL are significantly lower than all other simulations (Fig. 8b) due to a particularly large Brewer-Dobson circulation strength and trend (Oman et al., 2010b). This can also be seen by comparing the MMT of the reference simulation (black line and grey shaded area) to the timeseries of w^* in SOCOL (green line) in Fig. 7. An attribution of ozone changes in the tropical lower stratosphere to changes in ODSs and GHGs is shown in Fig. 6b. In the lower stratosphere in the tropics ozone shows little response to ESC through the 20th and 21st centuries as seen from the fGHG trace. The ~25% decrease in ozone from 1960 to 2100 in the reference scenario results from GHG induced changes to stratospheric dynamics as evidenced by the fixed ODS scenario. Note also that in the fixed ODS simulation, ESC decreases with time in response to these circulation changes. As in the upper stratosphere, the response of ozone to ODSs and GHGs is almost linearly additive as shown by the close agreement between the REF and grey traces in Fig. 6b. In this panel the multi-model mean was calculated using the CCSRNIES, CMAM, MRI and WACCM models (see individual models in Figs. SM6 to SM15 in the supplementary material). SOCOL was excluded since in their fGHG simulation SSTs were not fixed at the 1955 to 1964 climatological mean but rather followed those in the REF simulation with the result that in their fGHG simulation ozone behaves similarly to their REF simulation. This indicates that ozone in the tropical lower stratosphere responds primarily to the underlying SSTs with only a small contribution from the in situ effects of GHG radiative forcing. ULAQ was also excluded for the reasons outlined above (see also supplementary online material).

**'Multi-model
assessment of ozone
return dates and
recovery**V. Eyring et al.

Title Page

Abstract

Introduction

Conclusions

References

Tables

Figures



Back

Close

Full Screen / Esc

Printer-friendly Version

Interactive Discussion



'Multi-model assessment of ozone return dates and recovery

V. Eyring et al.

Title Page

Abstract

Introduction

Conclusions

References

Tables

Figures

⏪

⏩

◀

▶

Back

Close

Full Screen / Esc

Printer-friendly Version

Interactive Discussion



The evolution of tropical column ozone (Fig. 8b) depends on the balance between the increase in upper stratospheric concentrations and the decrease in lower stratospheric concentrations, and as a result the projected changes are in general small compared to extra-tropical regions in the reference simulations (less than 8 DU, see Table 4). In the MMT calculated from the 16 CCMs' reference simulations, there is a general decline from the start of the integrations until about 2001, followed by a gradual increase until about 2050 with 44% of the simulated ozone lost since 1980 recovered by 2025 and 70% by 2050 in the multi-model mean (Table 4). After 2050, column ozone amounts decline slightly again toward the end of the century. Increased tropical upwelling is one of the largest drivers of this (see Fig. 7 as well as Shepherd, 2008; Li et al., 2009). This is confirmed by the similarity of the REF and fODS simulations in Fig. 8b after 2050. In the fGHG upper stratospheric tropical ozone is consistently lower than in REF (Fig. 5a) while tropical upwelling is not increasing except for SOCOL (Fig. 7), and consequently lower stratospheric tropical ozone is higher than in REF and remains nearly constant in fGHG (Fig. 5b). Consistently, the MMT of tropical column ozone in fGHG is higher than REF at the end of the 21st century and returns to its 1980 values around 2060 (Fig. 9b). A comparison of the REF, fODS and fGHG simulations for tropical total column ozone is also shown, using a different format, in Fig. 6c with the multi-model mean calculated from CCSRNIES, CMAM, MRI, and WACCM. Interestingly, unlike ozone at 5 and 50 hPa in the tropics, total column ozone shows deviations away from linear additivity demonstrated by the lack of coincidence of the orange and yellow traces in Fig. 6c. The reasons for this breakdown in linear additivity in tropical total column ozone are not yet clear.

4.2 Midlatitude ozone

The dominant factors that affect the long-term evolution of ozone in the midlatitude lower stratosphere are transport and decreasing halogen concentrations (Shepherd, 2008; Li et al., 2009). In the upper midlatitude stratosphere, which is mainly photochemically controlled, GHG-induced cooling of the stratosphere that slows chemical

destruction rates and leads to an increase in ozone are the dominant factors, while increases in N_2O and CH_4 appear to play a minor role in upper stratospheric ozone depletion under the SRES A1b GHG scenario (Eyring et al., 2007; Oman et al., 2010a).

Overall, the projected evolution of midlatitude upper stratospheric ozone is very similar to that in the tropics (Chapter 9 of SPARC CCMVal, 2010), and in the SRES A1b GHG scenario the evolution there is characterized by increasing ozone throughout the 21st century (Fig. 2c, e) due to GHG induced cooling (Fig. 3c,d). In the lower stratosphere the evolution of midlatitude ozone differs from that in the tropics (compare panel b in Fig. 2 with panels d and f), and rather than a steady decrease in ozone, first a decrease is simulated between 1960 and 2000, which is then followed by a steady increase throughout the 21st century. As in the tropics, changes in transport also play a role in the ozone evolution in midlatitudes but here the increase in the meridional circulation could lead to an increase rather than a decrease in ozone. Inter-hemispheric differences in changes in transport could explain the difference in the SH compared to the NH, since the increase in stratospheric circulation transports more ozone into NH midlatitudes lower stratosphere than in the SH (Shepherd, 2008; Li et al., 2009) and since in the SH the mixing of ozone poor air from the ozone hole into midlatitudes could also contribute. These inter-hemispheric differences are also evident in the MMT of lower stratospheric midlatitude ozone in the fGHG simulation which is slightly lower than in REF in the NH (see Fig. 5d, f). However, differences between fGHG and REF are generally small. The temperature evolution in the midlatitude lower stratosphere is similar to that in the tropics (compare panel b in Fig. 3 with panels d and f), though the temperature responds more to changes in ODSs through ODS induced changes in ozone (concluded by the larger difference of fODS and REF in the midlatitudes), in particular in the SH midlatitudes, consistent with previous studies which have shown a substantial contribution from ozone depletion to observed upper stratospheric cooling (WMO, 2007; Shepherd and Jonsson, 2008).

Because ozone averaged over mid-latitudes first decreases until around 2000 and then increases again in the upper and lower stratosphere over the 21st century, a sim-

**'Multi-model
assessment of ozone
return dates and
recovery**V. Eyring et al.

[Title Page](#)[Abstract](#)[Introduction](#)[Conclusions](#)[References](#)[Tables](#)[Figures](#)[Back](#)[Close](#)[Full Screen / Esc](#)[Printer-friendly Version](#)[Interactive Discussion](#)

and an 8.1% total column ozone reduction over southern midlatitudes over this period. In both hemispheres, as ESC decreases, total column ozone does not simply retrace the 1960–2000 path, but shows systematically elevated ozone through the 21st century. As a result, over NH midlatitudes total column ozone returns to 1980 values in the early 2020s, well before ESC returns to its 1980 value in the late 2040s. Similarly, over southern midlatitudes total column ozone returns to 1980 values in the mid-2030s (a decade later than in the northern hemisphere), and well before ESC returns to its 1980 value in the late 2040s. It is clear from the fODS scenario (blue traces in Fig. 10), that the elevated ozone through the 21st century results from GHG induced stratospheric cooling. The fODS simulations also show ESC decreasing with time even though ODSs are fixed at 1960 values. This results from the increasing strength of the Brewer-Dobson circulation through the 21st century and a resultant decrease in the time available to photolyze ODSs in the upper stratosphere and mesosphere. It is also clear from the REF and fODS traces in Fig. 10 that by 2100 total column ozone over midlatitudes is still being influenced by ESC. In both the NH and SH midlatitudes the effects of ODSs and GHGs on column ozone are approximately linearly additive (agreement of black and yellow traces in Fig. 10b and c).

4.3 Polar ozone in spring

In the Antarctic (60°–90° S) in spring, the general characteristics of ozone evolution in the CCMVal-2 reference simulation are similar in all CCMs and similar to the CCM projections shown in Eyring et al. (2007). Lower stratospheric ozone (Fig. 2h) and total column ozone (Fig. 8f) are dominated by responses to ODSs, resulting in peak ozone depletion around 2000 (~80 DU lower than its 1980 value, see Table 4), followed by a slow and steady increase until 2100. By the year 2025, 46% of the ozone loss since 1980 is projected to rebuild, and 94% by 2050. By the end of the 21st century, Antarctic spring ozone will have higher concentrations than in 1980 (+51 DU, 163%), but still be lower than in 1960 (–9.7 DU, 93%). The dominant role of ozone responding to ODSs in Antarctic spring is well known (Eyring et

**'Multi-model
assessment of ozone
return dates and
recovery**

V. Eyring et al.

Title Page

Abstract

Introduction

Conclusions

References

Tables

Figures



Back

Close

Full Screen / Esc

Printer-friendly Version

Interactive Discussion



al., 2007; Chapter 9 of SPARC CCMVal, 2010) and is further confirmed here by the large difference between the fixed ODS simulations and the reference simulations (Fig. 2h and 8f) compared to the relatively small difference between the reference and the fixed GHG simulations (Figs. 5h and 9f). Attribution of Antarctic column ozone changes to ODSs and GHGs is shown in Fig. 10d with the multi-model mean calculated as for midlatitude total column ozone (see individual models in Figs. SM21 to SM25 in the supplementary material, <http://www.atmos-chem-phys-discuss.net/10/11659/2010/acpd-10-11659-2010-supplement.pdf>). The reference simulation shows total column ozone decreasing from 1960 to 2000 with a 52 DU/ppb sensitivity to ESC, leading to a 36.7% decrease in total column ozone over this period. Unlike the midlatitudes and Arctic (Fig. 10a–c), the total column ozone evolution over Antarctica (Fig. 10d) shows almost no sensitivity to changes in GHGs with the return path (21st century) closely tracking the outbound path (20th century). This is corroborated by the fixed ODS simulation which shows almost no change in ozone in response to increasing GHGs. Since ozone shows almost no response to GHGs in this region, assessing the additivity of the simulations is not appropriate.

In the Arctic (60°–90° N) in spring, lower stratospheric ozone (Fig. 2g) and total column ozone (Fig. 8e) follow a similar evolution to spring-time Antarctic ozone, with however smaller ozone losses during the peak ozone depletion period (~25 DU smaller than its 1980 value, see Table 4) and with ozone increasing significantly above 1980 and even 1960 values at the end of the century in the reference simulation. Most of the simulations using the fixed ODS scenarios show a steady increase in Arctic ozone over the 21st century, likely related to the increases in the strength of the Brewer-Dobson circulation and enhanced stratospheric cooling associated with increases in GHGs. In the fixed GHG simulations, depletion of ozone in the Arctic is much greater than in the reference simulations (Fig. 9g), with a much later date of return of ozone column amounts to 1980 values when the counterbalancing effects of GHGs are excluded. The attribution of Arctic ozone changes to GHG and ODS changes is further illustrated in Fig. 10a, where an attribution of total column ozone changes over the

**'Multi-model
assessment of ozone
return dates and
recovery**V. Eyring et al.

[Title Page](#)[Abstract](#)[Introduction](#)[Conclusions](#)[References](#)[Tables](#)[Figures](#)[Back](#)[Close](#)[Full Screen / Esc](#)[Printer-friendly Version](#)[Interactive Discussion](#)

Arctic to changes in ODSs and GHGs is shown for the multi-model mean calculated as for midlatitude total column ozone (see individual models in Figs. SM16 to SM20 in the supplementary material, supplementpdf). The reference simulation shows total column ozone decreasing from 1960 to 2000 with a -14 DU/ppb sensitivity to ESC, less than the -16 DU/ppb sensitivity observed over southern midlatitudes. The increase in ESC from 1.1 ppb in 1960 to 3.5 ppb in 2000 leads to a 7.5% decrease in total column ozone over this period. As for the midlatitudes, total column ozone over the Arctic is elevated above what would be expected from changes in ESC by stratospheric cooling and changes to the Brewer-Dobson circulation induced by increasing GHGs – see fixed ODS simulation. Through the latter half of the century the system shows a high degree of linear additivity (close agreement of black and yellow traces in Fig. 10a). As discussed in Butchart et al. (2010) and Chapter 4 of SPARC CCMVal (2010), in the models the extra radiative cooling from growing amounts of GHGs is approximately balanced by a concomitant increase in the adiabatic warming through increased polar downwelling with the net effect being a near zero temperature trend in the Arctic winter lower stratosphere. A small trend (-1 K from 2000 to 2100) is simulated in the extended set of CCMVal-2 models in March (Fig. 3g). However, it is also important to note that there is a very large spread between the fODS simulations, with some models simulating a slight increase in temperature in the Arctic by 2100. The large spread in the impact of GHG changes on Arctic temperature is likely to be related to changes in dynamical heating of the Arctic linked to GHG changes. Previous studies using stratospheric climate models have shown that the response to GHG changes can be very different between models with different horizontal resolution (Bell et al., 2010) and that these changes are related to changes in Arctic dynamical heating. The impact of ozone depletion and recovery on Arctic temperatures can be diagnosed from the fGHG runs in Fig. 4g. Arctic temperatures are close to their 1960 values by 2100 in this simulation and the temperatures from fODS and fGHG appear to be additive.

**'Multi-model
assessment of ozone
return dates and
recovery**V. Eyring et al.

[Title Page](#)[Abstract](#)[Introduction](#)[Conclusions](#)[References](#)[Tables](#)[Figures](#)[Back](#)[Close](#)[Full Screen / Esc](#)[Printer-friendly Version](#)[Interactive Discussion](#)

5 Ozone return dates and ozone recovery

Two distinct milestones in the future evolution of ozone, namely the return of ozone to historical values and the full recovery of ozone from the effects of ODSs (WMO, 2007) are assessed and compared in the reference simulations (see also Introduction). Ozone return dates to 1980 values are derived from the 1960 and 1980 baseline-adjusted reference simulation (REF) ozone time series. The selection of baseline adjustment has little effect on the results since the 1980 return date remains unaffected and the uncertainty on that date increases by at most 3 years when shifting from 1980 to 1960 baseline adjusted time series (see Fig. 1 for illustration of the global total column ozone return dates and Table 3). The robustness of the 1980 return date to baseline adjustment selection means that 1980 ozone return dates calculated from the 1980 baseline-adjusted time series can be directly compared to the date of full ozone recovery which must be calculated from the 1960 baseline-adjusted time series. This is necessary because full recovery of ozone from the effects of ODSs is evaluated as when ozone is no longer significantly affected by ODSs (WMO, 2007), i.e. as the fODS and REF simulations converge. Here, we apply the student's t-test to test whether the multi-model means calculated from the fODS and REF simulations are from the same population, and use this to quantify the likelihood that full recovery has occurred. The sample variance σ^2 for REF and fODS in the t-test is obtained from the TSAM 95% prediction interval I , following the relation $\sigma^2 = (I \text{ SQRT}(n)/2 \times 1.96)^2$, where n is the number of models in the multi-model mean. As in IPCC (2007), the following terms are used to indicate the assessed likelihood: if the confidence level from the t-test is >95%, then it is extremely likely that full ozone recovery has occurred (within 2σ confidence), if it is >90% it is very likely that it has occurred, while if it is >66% it is likely that it has occurred (within 1σ confidence). For values between 33% and 66% probability it is about as likely as not and for values <33% it is unlikely that full recovery of ozone has occurred.

'Multi-model assessment of ozone return dates and recovery

V. Eyring et al.

Title Page

Abstract

Introduction

Conclusions

References

Tables

Figures



Back

Close

Full Screen / Esc

Printer-friendly Version

Interactive Discussion



**'Multi-model
assessment of ozone
return dates and
recovery**

V. Eyring et al.

[Title Page](#)[Abstract](#)[Introduction](#)[Conclusions](#)[References](#)[Tables](#)[Figures](#)[⏪](#)[⏩](#)[◀](#)[▶](#)[Back](#)[Close](#)[Full Screen / Esc](#)[Printer-friendly Version](#)[Interactive Discussion](#)

Figure 11 shows the date of return to 1960 (upper panel) and 1980 (lower panel) total column ozone compared to the return date of Cl_y at 50 hPa and ESC at 50 hPa for the annual average (global, tropical and midlatitude) and spring (polar) total ozone column derived from the MMT (large triangles) of the CCMVal-2 reference simulations (16 CCMs) in each latitude band. Note that the return dates differ slightly from return dates derived from the MMT in Figs. 8 and 9 where in the multi-model mean only 7 and 5 out of the 16 CCMs are considered, respectively. They also differ from Austin et al. (2010) and Chapter 9 of SPARC CCMVal (2010) who used only 15 out of the 16 CCMs used here. The MMT ESC at 50 hPa is calculated as $Cl_y + 60 \times Br_y$ except for one model (E39CA) where Cl_y instead of ESC was used. This model does not have available separate information about Br_y , since it applies a bromine parameterisation (see Appendix of Stenke et al. (2009)).

There is no consensus between CCMs on whether tropical total column ozone will return to 1980 values, with some models showing ozone increasing slightly above 1980 values by the second half of the 21st century and others with ozone remaining below 1980 values through the 21st century (see Austin et al., 2010; Chapter 9 of SPARC CCMVal, 2010). This is reflected by the large error bar derived from the 95% TSAM confidence interval which extends from around 2030 to beyond the end of the century. However, unlike in the above mentioned studies which included 15 out of the 16 CCM REF simulations used here, the addition of one model (EMAC-FUB) in this study, a model which returns to 1980 values earlier than the MMT in the tropics, causes the MMT to return to its 1980 value in 2049. Note also that tropical column ozone derived from the subset of 9 CCMs in Fig. 8b does also not return to its 1980 value, showing again that the tropical ozone return date is not a robust quantity across the CCMs. However, there is a consensus in all CCMs that tropical column ozone will not return to 1960 values, i.e. even when stratospheric halogens return to historical (pre-1960) values tropical column ozone will remain below its historical values due to the increase in tropical upwelling (see Fig. 11a and Chapter 9 of SPARC CCMVal, 2010). In contrast, Cl_y and ESC in the tropical region return to 1980 values faster than in all other regions

(Fig. 11b) with only minor difference between them. By the end of the century, it is likely (~82%) that full recovery of tropical column ozone from the effects of ODSs will have occurred, while the 1σ confidence level (66%) is projected to be reached already ~2070 (see Table 5). Column ozone in the tropics is projected to decrease again in the 2nd half of the 21st century due to climate change (see Section 4.1). In the upper tropical stratosphere, ozone returns to 1980 values at ~2020 which is faster than in other regions (see Fig. 2a), while it is about as likely as not (~44%) that full ozone recovery has occurred by the end of the 21st century (see Table 5). In the lower tropical stratosphere however, ozone never returns to its 1980 values. That said, because ozone in this region is little affected by ODSs, the recovery of ozone from ODS effects is identified above the 1σ confidence level (66%) throughout the entire 21st century, and above the 2σ confidence level (95%) from 2040 onwards.

In the midlatitude NH, total column ozone returns to 1980 values around 2020 (within a bounded range of 2017 to 2027, see Fig. 11b and Table 3). This is the fastest return out of all regions considered here, confirming previous studies (e.g., Shepherd, 2008; Austin et al., 2010; Chapter 9 of SPARC CCMVal, 2010). While the qualitative evolution is the same in both hemispheres in the CCMs, the midlatitude anomalies are larger in the SH and the return of midlatitude column ozone to 1980 values therefore occurs later in the SH (~ 2037 within a bounded range of 2031 to 2043) than in the NH. The difference in the date of return to 1980 values appears to be due to inter-hemispheric difference in changes in transport, see discussion in Sect. 4.2. In all CCMs the return of total column ozone to 1980 values in the midlatitudes occurs before that of Cl_y and ESC (~2050 in both hemispheres). In contrast, in the NH midlatitudes it is likely (72%) that full recovery of total column ozone has occurred by the end of the 21st century, while it is about as likely as not (61%) in the SH midlatitudes (Fig. 8c,d and Table 5). In both hemispheres, midlatitude column ozone also returns to 1960 values, but significantly later than when it returns to 1980 values (~2058 in SH and ~2032 in NH). In the midlatitude upper stratosphere, ozone returns to 1980 values ~2030 (see Fig. 2c,e), while in both hemispheres it is unlikely that full ozone recovery has occurred by the end

**'Multi-model
assessment of ozone
return dates and
recovery**V. Eyring et al.

[Title Page](#)[Abstract](#)[Introduction](#)[Conclusions](#)[References](#)[Tables](#)[Figures](#)[⏪](#)[⏩](#)[◀](#)[▶](#)[Back](#)[Close](#)[Full Screen / Esc](#)[Printer-friendly Version](#)[Interactive Discussion](#)

of the 21st century (see Table 5). In the midlatitude lower stratosphere, ozone returns to its 1980 values ~ 2055 , while full ozone recovery at the 1σ confidence interval is reached ~ 2040 in the NH and ~ 2070 in the SH. By the end of the century, it is likely that full recovery has occurred in the NH and SH midlatitude lower stratosphere ($\sim 89\%$ and 83% , respectively).

As discussed in Sect. 4.3, Antarctic spring ozone column evolution is dominated by ODSs, and in this region ozone return dates are very similar to Cl_y and ESC return dates and occur later than in all other regions. Column ozone is therefore projected to return to its 1980 values around 2052 (within a bounded range of 2047 to 2059, see Table 3 and Fig. 11b). There is however a spread in the magnitude of the changes among the CCMs which can also be seen by the 95% confidence interval of the MMT (Fig. 8f) and by the uncertainty in the time of return to 1980 values (between 2045 and 2063). This spread is closely linked to the spread in simulated Cl_y (Chapter 9 of SPARC CCMVal, 2010). On the other hand, it is about as likely as not (62%) that full ozone recovery in the reference simulations has occurred until the end of the 21st century (compare fODS with REF in Fig. 8f, see also Table 5), and column ozone has also not returned to its 1960 values by then (Fig. 11a). In contrast, in the Arctic, total column ozone is projected to return to its 1980 values already around 2027 (within a bounded range of 2023 to 2031), which is much earlier than when Cl_y and ESC return to 1980 values in this region, and it is also projected to return to its 1960 values (~ 2050). Full recovery of total column ozone at the 1σ confidence level (66%) in the Arctic is reached earlier than in all other regions (~ 2035) and it is likely that ozone has fully recovered ($\sim 85\%$) by the end of the century (Fig. 8e and Table 5). Global total column ozone returns to its 1980 values around 2034 (within a bounded range of 2028 to 2041), which is earlier than global Cl_y or ESC at 50 hPa (Fig. 11b), while it is about as likely as not (55%) that full ozone recovery has occurred by the end of the century (Fig. 8a).

Overall, column ozone returns to its 1980 values in all regions, with largest uncertainty in the ozone return date estimate in the tropics, while by 2100 it returns to its 1960 values only in the midlatitudes and in the Arctic, but not over Antarctica and not

'Multi-model assessment of ozone return dates and recovery

V. Eyring et al.

[Title Page](#)[Abstract](#)[Introduction](#)[Conclusions](#)[References](#)[Tables](#)[Figures](#)[⏪](#)[⏩](#)[◀](#)[▶](#)[Back](#)[Close](#)[Full Screen / Esc](#)[Printer-friendly Version](#)[Interactive Discussion](#)

**'Multi-model
assessment of ozone
return dates and
recovery**

V. Eyring et al.

Title Page

Abstract

Introduction

Conclusions

References

Tables

Figures

⏪

⏩

◀

▶

Back

Close

Full Screen / Esc

Printer-friendly Version

Interactive Discussion



in the tropics. It is not likely that full recovery of ozone has occurred by the end of the century in any of the upper stratosphere regions. In the tropical lower stratosphere (50 hPa), however, it is very likely that full ozone recovery from ODSs has occurred by the end of the 21st century while it is likely that it occurred also over midlatitudes. For total column ozone, full ozone recovery is not reached at the 2σ confidence level in any of the regions, while at the 1σ level it is projected to occur ~ 2035 in the Arctic, ~ 2065 at NH midlatitudes, and ~ 2069 in the tropics, but not in the SH midlatitudes and not over Antarctica. In the SH midlatitudes and in the Antarctic it is still not likely that ozone has fully recovered from ODSs by the end of the century (61% and 56%, respectively). The larger set of models used here confirms the overall findings of Waugh et al. (2009) who assessed ozone recovery within GEOSCCM.

6 Discussion and conclusions

In this paper projections of stratospheric ozone throughout the 21st century have been examined from a suite of chemistry-climate models (CCMs). In the future reference simulations (REF) that were provided by 16 CCMs, surface halogenated Ozone Depletion Substances (ODSs) are prescribed according to the adjusted A1 halogen scenario of WMO (2007) and long-lived greenhouse gases (GHG) according to the SRES (Special Report on Emission Scenarios) GHG scenario A1b (IPCC, 2000). The reference simulations were compared to sensitivity simulations with either ODSs or GHGs concentrations fixed at 1960 levels, which were performed by a subset of models (9 and 8 CCMs, respectively) to disaggregate the drivers of projected ozone changes. These simulations were also used to assess the two distinct milestones of ozone returning to historical values (ozone return dates) and ozone no longer being discernibly influenced by ODSs (full ozone recovery). This study therefore extends the analysis on ozone projections of Chapter 9 of SPARC CCMVal (2010) and Austin et al. (2010) and the study by Waugh et al. (2009) who assessed full ozone recovery using a single model.

**'Multi-model
assessment of ozone
return dates and
recovery**V. Eyring et al.

[Title Page](#)[Abstract](#)[Introduction](#)[Conclusions](#)[References](#)[Tables](#)[Figures](#)[⏪](#)[⏩](#)[◀](#)[▶](#)[Back](#)[Close](#)[Full Screen / Esc](#)[Printer-friendly Version](#)[Interactive Discussion](#)

In the tropical and midlatitude upper stratosphere ozone in the reference simulations decreases between 1960 and 2000 in response to increasing equivalent stratospheric chlorine (ESC), followed by a steady increase until the end of the 21st century, confirming previous results (e.g. Waugh et al., 2009; Oman et al., 2010b). However, as ESC decreases from 2000 to 2100 ozone does not simply retrace the 1960-2000 path but, as a result of GHG induced stratospheric cooling, shows systematically elevated ozone through the 21st century such that ozone returns to 1980 values in the 2020s well before ESC returns to its 1980 value in the mid-2050s. By 2100 ozone is still being influenced by ESC and hence it is not likely that full recovery of ozone in this region of the atmosphere has occurred. In the tropical lower stratosphere, a robust result simulated by CCMs is a steady decline of ozone from 1960 to 2100 due to increased tropical upwelling that has also been shown in previous studies using a smaller subset of CCMs (e.g. Eyring et al., 2007; WMO, 2007; Butchart et al., 2010; SPARC CCMVal, 2010). Ozone in the simulation with fODS is nearly identical to REF, confirming again that in the lower tropical stratosphere ozone shows little response to ODSs. Although ozone decreases continuously from 1960 to 2100, the tropical lower stratosphere is together with the Arctic lower stratosphere the only region where ozone has very likely fully recovered from the effects of ODSs. In the lower midlatitude stratosphere the evolution differs from that in the tropics, and rather than a steady decrease of ozone, first a decrease of ozone is simulated between 1960 and 2000, which is then followed by a steady increase throughout the 21st century. Ozone in the lower stratosphere midlatitudes returns to its 1980 levels ~2045 in the NH and ~2055 in the SH, and full ozone recovery is likely reached by 2100 in both hemispheres.

Projected tropical total column ozone changes are in general small compared to extra-tropical regions (less than 8 DU in the reference simulations). Model uncertainty in tropical column evolution is high (see also Charlton-Perez et al., 2010), mostly related to the large spread that is simulated in the magnitude of tropical upwelling among the CCMVal-1 and CCMVal-2 models (see also Butchart et al., 2010 and Chapter 4 of SPARC CCMVal 2010). Unlike in the previous CCMVal-2 study by Austin et al. (2010)

**'Multi-model
assessment of ozone
return dates and
recovery**

V. Eyring et al.

Title Page

Abstract

Introduction

Conclusions

References

Tables

Figures

⏪

⏩

◀

▶

Back

Close

Full Screen / Esc

Printer-friendly Version

Interactive Discussion



and Chapter 9 of SPARC CCMVal (2010) that used 15 out of the 16 CCMs included here, the addition of one CCM caused the multi-model mean of the 16 CCMs to return to its 1980 value in the tropics, showing that the ozone return date is not a robust quantity in the tropics, given the large spread that is simulated by the individual models.

5 Over northern midlatitudes total column ozone returns to 1980 values in the mid-2020s in the reference simulations, well before ESC returns to its 1980 value in the late 2040s. Similarly, over southern midlatitudes total column ozone returns to 1980 values in the mid-2030s (a decade later than in the northern hemisphere), and well before ESC returns to its 1980 value in the early 2050s. By 2100 total column ozone over midlatitudes
10 is still influenced by ESC and full recovery of column ozone has likely occurred in the NH midlatitudes while it has not likely occurred in the SH midlatitudes.

Unlike the midlatitudes and Arctic, the total column ozone evolution over Antarctica shows almost no sensitivity to changes in GHGs with the return path (21st century) closely tracking the outbound path (20th century). By the end of the century it is still
15 not likely that total column ozone has fully recovered from ODSs. In the Arctic (60°–90° N) in spring, total column ozone follows a similar evolution to spring-time Antarctic ozone, with however smaller ozone losses during the peak ozone depletion period and with ozone increasing significantly above 1980 and even 1960 values at the end of the century in the reference, but not in the fixed GHG simulation, indicating that
20 climate change plays a significant role. As for the midlatitudes, total column ozone over the Arctic is elevated above what would be expected from changes in ESC by stratospheric cooling induced by increasing GHGs. In the Arctic it is likely (>66%) that full recovery of total column ozone from the effects of ODS will have occurred by about 2035. However, at no time before 2100 is it likely (>90%) that full recovery will have
25 occurred.

It is important to note that the future ozone evolution as well as the two milestones of ozone returning to its historical values and ozone recovering from the influence of ODSs have been studied here using a single GHG scenario. However, the SRES A1b scenario that was used in the CCMVal-2 reference simulations is only one plausible

**'Multi-model
assessment of ozone
return dates and
recovery**

V. Eyring et al.

Title Page

Abstract

Introduction

Conclusions

References

Tables

Figures

⏪

⏩

◀

▶

Back

Close

Full Screen / Esc

Printer-friendly Version

Interactive Discussion



GHG scenario for the future (IPCC, 2000; Moos et al., 2008). Given the importance of GHG induced changes on stratospheric temperatures, chemistry, circulation and transport on the evolution of ozone through the 21st century shown here and in previous studies, it is likely that the importance of the factors affecting ozone and the resulting future ozone evolution will be different under a different GHG scenario (see also Charlton-Perez et al., 2010; Eyring et al., 2010; Oman et al., 2010a). Likewise, the future ozone evolution would be different for different ODSs scenarios (see for example the extreme “world avoided” scenarios that were studied by Morgenstern et al. (2008) and Newman et al., 2009). In addition, since all the CCMs used here are forced by specifying mixing ratios of ODSs at the surface rather than specifying emissions, the flux of halogen source gases entering the stratosphere is highly constrained and therefore the evolution of the ESC loading is expected to be similar in the CCMs (see Chapter 6 of SPARC CCMVal, 2010). In reality, surface source gases levels should be determined by emission fluxes and rates of loss processes which could increase the spread in modeled halogen loadings and hence in stratospheric ozone losses (Douglass et al., 2008). Other uncertainties in the ozone projections could stem from the neglect of additional bromine from very short-lived substances (VSLS) (Sinnhuber et al., 2005; Chapter 2 of WMO, 2007) which could result in a substantial fractional increase to the amount of bromine in the lowermost stratosphere as upwelling changes (Gettelman et al., 2009), with important consequences for ozone trends and the photochemical budget of ozone.

Acknowledgements. We thank NOAA GFDL (USA) and Meteo-France (France) for making the AMTRAC3 and CNRM-ACM reference simulations available for this analysis. We acknowledge the Chemistry-Climate Model Validation (CCMVal) Activity for WCRP’s (World Climate Research Programme) SPARC (Stratospheric Processes and their Role in Climate) project for organizing and coordinating the model data analysis activity, and the British Atmospheric Data Center (BADC) for collecting and archiving the CCMVal model output. We thank David. B. Stephenson (Mathematics Research Institute, University of Exeter, UK) for his work on the TSAM method. CCSRNIIES research was supported by the Global Environmental Research Found of the Ministry of the Environment of Japan (A-071) and the simulations were completed

with the super computer at CGER, NIES. The MRI simulation was made with the supercomputer at the National Institute for Environmental Studies, Japan. The MetOffice simulation was supported by the Joint DECC and Defra Integrated Climate Programme, DECC/Defra (GA01101).

References

- 5 Akiyoshi, H., Zhou, L. B., Yamashita, Y., Sakamoto, K., Yoshiki, M., Nagashima, T., Takahashi, M., Kurokawa, J., Takigawa, M., and Imamura, T.: A CCM simulation of the breakup of the Antarctic polar vortex in the years 1980–2004 under the CCMVal scenarios, *J. Geophys. Res.*, 114, D03103, doi:10.1029/2007JD009261, 2009.
- 10 Akiyoshi, H., Yamashita, Y., Sakamoto, K., Zhou, L. B., and Imamura, T.: Recovery of stratospheric ozone in calculations by the CCSR/NIES CCM under the CCMVal-REF2 scenario and a no-climate-change run, *J. Geophys. Res.*, submitted, 2010.
- Austin, J. and Wilson, R. J.: Sensitivity of polar ozone to sea surface temperatures and chemistry, *J. Geophys. Res.*, submitted, 2009.
- 15 Austin, J., Scinocca, J., Plummer, D., Oman, L., Waugh, D., Akiyoshi, H., Bekki, S., Braesicke, P., Butchart, N., Chipperfield, M., Cugnet, D., Dameris, M., Dhomse, S., Eyring, V., Frith, S., Garcia, R. R., Garny, H., Gettelman, A., Hardiman, S. C., Kinnison, D., Lamarque, J. F., Mancini, E., Marchand, M., Michou, M., Morgenstern, O., Nakamura, T., Pawson, S., Pitari, G., Pyle, J., Rozanov, E., Shepherd, T. G., Shibata, K., Stolarski, R., Teysstedre, H., Wilson, R. J., and Yamashita, Y.: The decline and recovery of total column ozone using a multi-model time series analysis, *J. Geophys. Res.*, submitted, 2010.
- 20 Bell, C. J., Gray, L. J., and Kettleborough, J.: Changes in Northern Hemisphere stratospheric variability under increased CO₂ concentrations, *Q. J. Roy. Meteor. Soc.*, submitted, 2010.
- Butchart, N., Scaife, A. A., Bourqui, M., de Grandpré, J., Hare, S. H. E., Kettleborough, J., Langematz, U., Manzini, E., Sassi, F., Shibata, K., Shindell, D., and Sigmond, M.: Simulations of anthropogenic change in the strength of the Brewer-Dobson circulation, *Clim. Dynam.*, 27(7–8), 727–741, doi:10.1007/s00382-006-0162-4, 2006.
- 25 Butchart, N., Cionni, I., Eyring, V., Shepherd, T. G., Waugh, D. W., Akiyoshi, H., Austin, J., Brühl, C., Chipperfield, M. P., Cordero, E., Dameris, M., Deckert, R., Dhomse, S., Frith, S. M., Garcia, R. R., Gettelman, A., Giorgetta, M. A., Kinnison, D. E., Li, F., Mancini, E., McLandress, C., Pawson, S., Pitari, G., Plummer, D. A., Rozanov, E., Sassi, F., Scinocca,
- 30

'Multi-model assessment of ozone return dates and recovery

V. Eyring et al.

Title Page

Abstract

Introduction

Conclusions

References

Tables

Figures

⏪

⏩

◀

▶

Back

Close

Full Screen / Esc

Printer-friendly Version

Interactive Discussion



**'Multi-model
assessment of ozone
return dates and
recovery**

V. Eyring et al.

Title Page

Abstract

Introduction

Conclusions

References

Tables

Figures

⏪

⏩

◀

▶

Back

Close

Full Screen / Esc

Printer-friendly Version

Interactive Discussion



J. F., Shibata, K., and Tian, W.: Chemistry-climate model simulations of 21st century stratospheric climate and circulation changes, *J. Clim.*, in press, <http://journals.ametsoc.org/doi/abs/10.1175/2010JCLI3404.1>, 2010.

Charlton-Perez, A. J., Hawkins, E., Eyring, V., et al.: Quantifying uncertainty in projections of stratospheric ozone over the 21st century, *Atmos. Chem. Phys.*, submitted, 2010.

Chipperfield, M. P. and Feng, W.: Comment on: “Stratospheric Ozone Depletion at northern mid-latitudes in the 21st century: The importance of future concentrations of greenhouse gases nitrous oxide and methane”, *Geophys. Res. Lett.*, 30, 1389, doi:10.1029/2002GL016353, 2003.

Deckert, R. and Dameris, M.: Higher tropical SSTs strengthen the tropical upwelling via deep convection, *Geophys. Res. Lett.*, 35, L10813, doi:10.1029/2008GL033719, 2008a.

Deckert, R. and Dameris, M.: From ocean to stratosphere, *Science*, 322, 5698, doi:10.1126/science.1163709, 2008b.

deGrandpre, J., Beagley, S. R., Fomichev, V. I., Griffioen, E., McConnell, J. C., Medvedev, A. S., and Shepherd, T. G.: Ozone climatology using interactive chemistry: Results from the Canadian Middle Atmosphere Model, *J. Geophys. Res.*, 105, 26475–26491, 2000.

Déqué, M.: Frequency of precipitation and temperature extremes over France in an anthropogenic scenario: model results and statistical correction according to observed values, *Global Planet. Change*, 57, 16–26, 2007.

Douglass, A. R., Stolarski, R. S., Schoeberl, M. R., Jackman, C. H., Gupta, M. L., Newman, P. A., Nielsen, J. E., and Fleming, E. L.: Relationship of loss, mean age of air and the distribution of CFCs to stratospheric circulation and implications for atmospheric lifetimes, *J. Geophys. Res.*, 113, D14309, doi:10.1029/2007JD009575, 2008.

Egorova, T., Rozanov, E., Zubov, V., Manzini, E., Schmutz, W., and Peter, T.: Chemistry-climate model SOCOL: a validation of the present-day climatology, *Atmos. Chem. Phys.*, 5, 1557–1576, 2005, <http://www.atmos-chem-phys.net/5/1557/2005/>.

Eyring, V., Harris, N. R. P., Rex, M., Shepherd, T. G., Fahey, D. W., Amanatidis, G. T., Austin, J., Chipperfield, M. P., Dameris, M., De F. Forster, P. M., Gettelman, A., Graf, H. F., Nagashima, T., Newman, P. A., Pawson, S., Prather, M. J., Pyle, J. A., Salawitch, R. J., Santer, B. D., and Waugh, D. W.: A strategy for process-oriented validation of coupled chemistry-climate models. *B. Am. Meteorol. Soc.*, 86, 1117–1133, 2005.

Eyring, V., N. Butchart, D. W. Waugh, H. Akiyoshi, J. Austin, S. Bekki, G. E. Bodeker, B. A. Boville, C. Brühl, M. P. Chipperfield, E. Cordero, M. Dameris, M. Deushi, V. E. Fioletov, S. M.

**'Multi-model
assessment of ozone
return dates and
recovery**

V. Eyring et al.

Title Page

Abstract

Introduction

Conclusions

References

Tables

Figures

◀

▶

◀

▶

Back

Close

Full Screen / Esc

Printer-friendly Version

Interactive Discussion



Frith, R. R. Garcia, A. Gettelman, M. A. Giorgetta, V. Grewe, L. Jourdain, D. E. Kinnison, E. Mancini, E. Manzini, M. Marchand, D. R. Marsh, T. Nagashima, P. A. Newman, J. E. Nielsen, S. Pawson, G. Pitari, D. A. Plummer, E. Rozanov, M. Schraner, T. G. Shepherd, K. Shibata, R. S. Stolarski, H. Struthers, W. Tian, and M. Yoshiki, Assessment of temperature, trace species and ozone in chemistry-climate model simulations of the recent past, *J. Geophys. Res.*, 111, D22308, doi:10.1029/2006JD007327, 2006.

Eyring, V., Waugh, D. W., Bodeker, G. E., Cordero, E., Akiyoshi, H., Austin, J., Beagley, S. R., Boville, B., Braesicke, P., Brühl, C., Butchart, N., Chipperfield, M. P., Dameris, M., Deckert, R., Deushi, M., Frith, S. M., Garcia, R. R., Gettelman, A., Giorgetta, M., Kinnison, D. E., Mancini, E., Manzini, E., Marsh, D. R., Matthes, S., Nagashima, T., Newman, P. A., Nielsen, J. E., Pawson, S., Pitari, G., Plummer, D. A., Rozanov, E., Schraner, M., Scinocca, J. F., Semeniuk, K., Shepherd, T. G., Shibata, K., Steil, B., Stolarski, R., Tian, W., and Yoshiki, M.: Multimodel projections of stratospheric ozone in the 21st century, *J. Geophys. Res.*, 112, D16303, doi:10.1029/2006JD008332, 2007.

Eyring, V., Chipperfield, M. P., Giorgetta, M. A., Kinnison, D. E., Manzini, E., Matthes, K., Newman, P. A., Pawson, S., Shepherd, T. G., and Waugh, D. W.: Overview of the New CCMVal Reference and Sensitivity Simulations in Support of Upcoming Ozone and Climate Assessments and the Planned SPARC CCMVal Report, *SPARC Newsletter No. 30*, 20–26, 2008.

Eyring, V., Cionni, I., Lamarque, J. F., Akiyoshi, H., Bodeker, G. E., Charlton-Perez, A. J., Frith, S. M., Gettelman, A., Kinnison, D. E., Nakamura, T., Oman, L. D., Pawson, S., and Yamashita, Y.: Sensitivity of 21st century stratospheric ozone to greenhouse gas scenarios, *Geophys. Res. Lett.*, submitted, 2010.

Fomichev, V. I., Jonsson, A. I., de Grandpré, J., Beagley, S. R., McLandress, C., Semeniuk, K., and Shepherd, T. G.: Response of the middle atmosphere to CO₂ doubling: Results from the Canadian Middle Atmosphere Model. *J. Clim.*, 20, 1121–1144, 2007.

Garcia, R. R. and Randel, W. J.: Acceleration of the Brewer-Dobson Circulation due to Increases in Greenhouse Gases, *J. Atmos. Sci.*, 65, 2731–2739, 2008.

Garcia, R. R., Marsh, D. R., Kinnison, D. E., Boville, B. A., and Sassi, F.: Simulation of secular trends in the middle atmosphere, 1950–2003, *J. Geophys. Res.*, 112, D09301, doi:10.1029/2006JD007485, 2007.

Garny, H., Dameris, M., and Stenke, A.: Impact of prescribed SSTs on climatologies and long-term trends in CCM simulations, *Atmos. Chem. Phys.*, 9, 6017–6031, 2009,

'Multi-model assessment of ozone return dates and recovery

V. Eyring et al.

Title Page

Abstract

Introduction

Conclusions

References

Tables

Figures

⏪

⏩

◀

▶

Back

Close

Full Screen / Esc

Printer-friendly Version

Interactive Discussion

<http://www.atmos-chem-phys.net/9/6017/2009/>.

Gottelman, A., Lauritzen, P. H., Park, M., and Kay, J. E.: Processes regulating short-lived species in the tropical tropopause layer, *J. Geophys. Res.*, 114, D13303, doi:10.1029/2009JD011785, 2009.

5 Haigh, J. D. and Pyle, J. A.: Ozone perturbation experiments in a two-dimensional circulation model, *Q. J. Roy. Meteorol. Soc.*, 108, 551–574, 1982.

IPCC (Intergovernmental Panel on Climate Change) (2000), Special report on emissions scenarios: a special report of Working Group III of the Intergovernmental Panel on Climate Change, Cambridge University Press, Cambridge, UK, 599 pp., 2000.

10 Jöckel, P., Tost, H., Pozzer, A., Brühl, C., Buchholz, J., Ganzeveld, L., Hoor, P., Kerweg, A., Lawrence, M. G., Sander, R., Steil, B., Stiller, G., Tanarhte, M., Taraborrelli, D., van Aardenne, J., and Lelieveld, J.: The atmospheric chemistry general circulation model ECHAM5/MESSy1: consistent simulation of ozone from the surface to the mesosphere, *Atmos. Chem. Phys.*, 6, 5067–5104, 2006, <http://www.atmos-chem-phys.net/6/5067/2006/>.

15 Jonsson, A. I., de Grandpré, J., Fomichev, V. I., McConnell, J. C., and Beagley, S. R.: Doubled CO₂-induced cooling in the middle atmosphere: Photochemical analysis of the ozone radiative feedback, *J. Geophys. Res.*, 109, D24103, doi:10.1029/2004JD005093, 2004.

Jourdain, L., Bekki, S., Lott, F., and Lefèvre, F.: The coupled chemistry-climate model LMDz-REPROBUS: description and evaluation of a transient simulation of the period 1980–1999, *Ann. Geophys.*, 26(6), 1391–1413, 2008.

20 Kärcher, B. and Lohmann, U.: A Parameterization of cirrus cloud formation: Homogeneous freezing of supercooled aerosols, *J. Geophys. Res.* 107(D2), 4010, doi:10.1029/2001JD000470, 2002.

Lamarque, J.-F., Kinnison, D. E., Hess, P. G., and Vitt, F. M.: Simulated lower stratospheric trends between 1970 and 2005: Identifying the role of climate and composition changes, *J. Geophys. Res.*, 113, D12301, doi:10.1029/2007JD009277, 2008.

25 Li, F., Austin, J., and Wilson, J.: The Strength of the Brewer-Dobson Circulation in a Changing Climate: Coupled Chemistry-Climate Model Simulation, *J. Climate*, 21, 40–57, 2008.

Li, F., Stolarski, R. S., and Newman, P. A.: Stratospheric ozone in the post-CFC era, *Atmos. Chem. Phys.*, 9, 2207–2213, 2009, <http://www.atmos-chem-phys.net/9/2207/2009/>.

30 McLandress, C., Jonsson, A. I., Plummer, D. A., Reader, M. C., Scinocca, J. F., and Shepherd, T. G.: Separating the effects of climate change and ozone depletion on the dynamics of the Southern Hemisphere stratosphere, *J. Clim.*, in revision, 2010.

'Multi-model assessment of ozone return dates and recovery

V. Eyring et al.

Title Page

Abstract

Introduction

Conclusions

References

Tables

Figures

◀

▶

◀

▶

Back

Close

Full Screen / Esc

Printer-friendly Version

Interactive Discussion

- Montzka, S. A., Butler, J. H., Hall, B. D., Mondeel, D. J., and Elkins, J. W.: A decline in tropospheric bromine, *Geophys. Res. Lett.*, 30, 1826, doi:10.1029/2003GL017745, 2003.
- Moss, T., Babiker, M., Brinkman, S., Calvo, E., Carter, T., Edmonds, J., Elgizouli, I., Emori, S., Erda, L., Hibbard, K., Jones, R., Kainuma, M., Kelleher, J., Lamarque, J.-F., Manning, M., Matthews, B., Meehl, G., Meyer, L., Mitchell, J., Nakic'enović, N., O'Neill, B., Pichs, T., Riahi, K., Rose, S., Runci, P., Stouffer, R., van Vuuren, D., Weyant, J., Wilbanks, T., van Ypersele, J. P., and Zurek, M.: Towards New Scenarios for Analysis of Emissions, Climate Change, Impacts, and Response Strategies., Intergovernmental Panel on Climate Change, Geneva, available online at: <http://www.aimes.ucar.edu/docs/>, 132 pp., 2008.
- Morgenstern, O., Braesicke, P., Hurwitz, M. M., O'Connor, F. M., Bushell, A. C., Johnson, C. E., and Pyle, J. A.: The World Avoided by the Montreal Protocol, *Geophys. Res. Lett.*, 35, L16811, doi:10.1029/2008GL034590, 2008.
- Morgenstern, O., Braesicke, P., O'Connor, F. M., Bushell, A. C., Johnson, C. E., Osprey, S. M., and Pyle, J. A.: Evaluation of the new UKCA climate-composition model. Part 1: The stratosphere. *Geosci. Model Dev.*, 1, 43–57, 2009.
- Morgenstern, O., Giorgetta, M. A., Shibata, K., Eyring, V., Waugh, D. W., Shepherd, T. G., Akiyoshi, H., Austin, J., Baumgaertner, A. J. G., Bekki, S., Braesicke, P., Brühl, C., Chipperfield, M. P., Cugnet, D., Dameris, M., Dhomse, S., Frith, S. M., Garny, H., Gettelman, A., Hardiman, S. C., Hegglin, M. I., Kinnison, D. E., Lamarque, J.-F., Mancini, E., Manzini, E., Marchand, M., Michou, M., Nakamura, T., Nielsen, J. E., Pitari, G., Plummer, D. A., Rozanov, E., Scinocca, J. F., Smale, D., Teysse, H., Toohey, M., Tian, W., and Yamashita, Y.: Review of the formulation of present-generation stratospheric chemistry-climate models and associated external forcings, *J. Geophys. Res.*, accepted, 2010.
- Newman, P. A., Oman, L. D., Douglass, A. R., Fleming, E. L., Frith, S. M., Hurwitz, M. M., Kawa, S. R., Jackman, C. H., Krotkov, N. A., Nash, E. R., Nielsen, J. E., Pawson, S., Stolarski, R. S., and Velders, G. J. M.: What would have happened to the ozone layer if chlorofluorocarbons (CFCs) had not been regulated?, *J. Atmos. Chem. Phys.*, 9, 2113–2128, 2009, <http://www.atmos-chem-phys.net/9/2113/2009/>.
- Nissen, K., Matthes, K., Langematz, U., and Mayer, B.: Towards a better representation of the solar cycle in general circulation models, *Atmos. Chem. Phys.*, 7, 5391–5400, 2007, <http://www.atmos-chem-phys.net/7/5391/2007/>.
- Oman, L., Waugh, D. W., Pawson, S., Stolarski, R. S., and Newman, P. A.: On the influence of anthropogenic forcings on changes in the stratospheric mean age, *J. Geophys. Res.*, 114,

**'Multi-model
assessment of ozone
return dates and
recovery**

V. Eyring et al.

Title Page

Abstract

Introduction

Conclusions

References

Tables

Figures

⏪

⏩

◀

▶

Back

Close

Full Screen / Esc

Printer-friendly Version

Interactive Discussion



D03105, doi:10.1029/2008JD010378, 2009.

Oman, L. D., Waugh, D. W., Kawa, S. R., Stolarski, R. S., Douglass, A. R., and Newman, P. A.: Mechanisms and feedback causing changes in upper stratospheric ozone in the 21st century, *J. Geophys. Res.*, 115, D05303, doi:10.1029/2009JD012397, 2010a.

5 Oman, L. D., Plummer, D., Waugh, D. W., Austin, J., Scinocca, J., Douglass, A. R., Salawitch, R. J., Akiyoshi, H., Bekki, S., Braesicke, P., Butchart, N., Chipperfield, M., Dhomse, S., Eyring, V., Frith, S., Garcia, R. R., Gettelman, A., Hardiman, S. C., Kinnison, D., Lamarque, J. F., Mancini, E., Marchand, M., Michou, M., Morgenstern, O., Pawson, S., Pitari, G., Peter, T., Pyle, J., Rozanov, E., Shepherd, T. G., Shibata, K., Stolarski, R., Teysedre, H., and Tian, W.: Multi-model assessment of the factors driving the ozone evolution over the 21st century, *J. Geophys. Res.*, submitted, 2010b.

10 Pawson, S., Stolarski, R. S., Douglass, A. R., Newman, P. A., Nielsen, J. E., Frith, S. M., and Gupta, M. L.: Goddard Earth Observing System chemistry-climate model simulations of stratospheric ozone-temperature coupling between 1950 and 2005, *J. Geophys. Res.*, 113, D12103, doi:10.1029/2007JD009511, 2008.

15 Pitari, G., Mancini, E., Rizi, V., and Shindell, D. T.: Impact of Future Climate and Emission Changes on Stratospheric Aerosols and Ozone, *J. Atmos. Sci.*, 59, 2002.

Portmann, R. W. and Solomon, S.: Indirect radiative forcing of the ozone layer during the 21st century, *Geophys Res. Lett.*, 34, L02813, doi:10.1029/2006GL028252, 2007.

20 Randeniya, L. K., Vohralik, P. F., and Plumb, I. C.: Stratospheric ozone depletion at northern mid latitudes in the 21st century: The importance of future concentrations of greenhouse gases nitrous oxide and methane, *Geophys. Res. Lett.*, 29(4), 1051, doi:10.1029/2001GL014295, 2002.

25 Ravishankara, A. R., Daniel, J. S., and Portmann, R. W.: Nitrous Oxide (N₂O): The Dominant Ozone-Depleting Substance Emitted in the 21st Century, *Science*, 326, 123–125, doi:10.1126/science.1176985, 2009.

Rosenfield, J. E., Douglass, A. R., and Considine, D. B.: The impact of increasing carbon dioxide on ozone recovery, *J. Geophys. Res.*, 107(D6), 4049, doi:10.1029/2001JD000824, 2002.

30 Schraner, M., Rozanov, E., Schnadt Poberaj, C., Kenzelmann, P., Fischer, A. M., Zubov, V., Luo, B. P., Hoyle, C. R., Egorova, T., Fueglistaler, S., Brönnimann, S., Schmutz, W., and Peter, T.: Technical Note: Chemistry-climate model SOCOL: version 2.0 with improved transport and chemistry/microphysics schemes, *Atmos. Chem. Phys.*, Atmos. Chem. Phys., 8, 5957–5974,

'Multi-model assessment of ozone return dates and recovery

V. Eyring et al.

Title Page

Abstract

Introduction

Conclusions

References

Tables

Figures

⏪

⏩

◀

▶

Back

Close

Full Screen / Esc

Printer-friendly Version

Interactive Discussion

2008, <http://www.atmos-chem-phys.net/8/5957/2008/>.

Scinocca, J. F., McFarlane, N. A., Lazare, M., Li, J., and Plummer, D.: Technical Note: The CCCma third generation AGCM and its extension into the middle atmosphere, *Atmos. Chem. Phys.*, 8, 7055–7074, 2008, <http://www.atmos-chem-phys.net/8/7055/2008/>.

5 Scinocca, J. F., Stephenson, D. B., Bailey, T. C., and Austin, J.: Estimates of past and future ozone trends from multi-model simulations using a flexible smoothing spline methodology, *J. Geophys. Res.*, submitted, 2010.

Shepherd, T. G.: Dynamics, Stratospheric Ozone, and Climate Change. *Atmos. Ocean*, 46, 117–138, 2008.

10 Shepherd, T. G. and A. I. Jonsson, On the attribution of stratospheric ozone and temperature changes to changes in ozone-depleting substances and well-mixed greenhouse gases, *Atmos. Chem. Phys.*, 8, 1435–1444, 2008

Shibata, K. and Deushi, M.: Long-term variations and trends in the simulation of the middle atmosphere 1980–2004 by the chemistry-climate model of the Meteorological Research Institute, *Ann. Geophys.*, 26, 1299–1326, 2008a, <http://www.ann-geophys.net/26/1299/2008/>.

15 Shibata, K. and Deushi, M.: Simulation of the stratospheric circulation and ozone during the recent past (1980–2004) with the MRI chemistry-climate model, CGER's Supercomputer Monograph Report Vol.13, National Institute for Environmental Studies, Japan, 154 pp., 2008b.

20 Sinnhuber, B.-M., Rozanov, A., Schoede, N., Afe, O. T., Richter, A., Sinnhuber, M., Wittrock, F., Burrows, J. P., Stiller, G. P., von Clarmann, T., and Linden, A.: Global observations of stratospheric bromine monoxide from SCIAMACHY, *Geophys. Res. Lett.*, 32, L20810, doi:10.1029/2005GL023839, 2005.

Stenke, A., Dameris, M., Grewe, V., and Garny, H.: Implications of Lagrangian transport for simulations with a coupled chemistry-climate model, *Atmos. Chem. Phys.*, 9, 5489–5504, 2009, <http://www.atmos-chem-phys.net/9/5489/2009/>.

25 SPARC CCMVal, SPARC CCMVal Report on the Evaluation of Chemistry-Climate Models, edited by: Eyring, V., Shepherd, T. G., Waugh, D. W., SPARC Report No. 5, WCRP-X, WMO/TD-No. X, <http://www.atmosp.physics.utoronto.ca/SPARC>, 2010.

30 Teyssèdre, H., Michou, M., Clark, H. L., Josse, B., Karcher, F., Olivie, D., Peuch, V.-H., Saint-Martin, D., Cariolle, D., Attié, J.-L., Nédélec, P., Ricaud, P., Thouret, V., van der A, R. J., Volz-Thomas, A., and Cheroux, F.: A new tropospheric and stratospheric Chemistry and Transport Model MOCAGE-Climat for multi-year studies: evaluation of the present-day climatology and

sensitivity to surface processes, Atmos. Chem. Phys., 7, 5815–5860, 2007,
<http://www.atmos-chem-phys.net/7/5815/2007/>.

Tian, W. and Chipperfield, M. P.: A new coupled chemistry-climate model for the stratosphere: the importance of coupling for future O₃-climate predictions, Q. J. Roy. Meteor. Soc., 131, 281–303, 2005.

Tian, W., Chipperfield, M. P., Gray, L. J., and Zawodny, J. M.: Quasi-biennial oscillation and tracer distributions in a coupled chemistry-climate model, J. Geophys. Res., 111, D20301, doi:10.1029/2005JD006871, 2006.

Waugh, D. W., Oman, L., Kawa, S. R., Stolarski, R. S., Pawson, S., Douglass, A. R., Newman, P. A., and Nielsen, J. E.: Impacts of climate change on stratospheric ozone recovery, Geophys. Res. Lett., 36, L03805, doi:10.1029/2008GL036223, 2009.

World Meteorological Organization (WMO)/United Nations Environment Programme (UNEP), Scientific Assessment of Ozone Depletion: 2006, World Meteorological Organization, Global Ozone Research and Monitoring Project, Report No. 50, Geneva, Switzerland, 2007.

ACPD

10, 11659–11710, 2010

**'Multi-model
assessment of ozone
return dates and
recovery**

V. Eyring et al.

Title Page

Abstract

Introduction

Conclusions

References

Tables

Figures

⏪

⏩

◀

▶

Back

Close

Full Screen / Esc

Printer-friendly Version

Interactive Discussion



'Multi-model assessment of ozone return dates and recovery

V. Eyring et al.

Title Page

Abstract

Introduction

Conclusions

References

Tables

Figures

⏪

⏩

◀

▶

Back

Close

Full Screen / Esc

Printer-friendly Version

Interactive Discussion

Table 1. A summary of the CCMs and simulations used in this study. REF is the future reference simulation, fODS is a simulation with fixed ODSs and fGHG a simulation with fixed GHGs. Further details on the models can be found in Morgenstern et al. (2010) and SPARC CCMVal (2010) as well as in the references given below. CCMs that contributed sensitivity simulations are highlighted in bold. $N \times$ REF means that the group provided N realizations of this simulation.

	CCM	Group and Location	Horiz. Res.	Upper level	REF	fODS	fGHG	References
1	AMTRAC3	GFDL, USA	~200 km	0.017 hPa	REF	–	–	Austin and Wilson (2009)
2	CAM3.5	NCAR, USA	$1.9^\circ \times 2.5^\circ$	3.5 hPa	REF	–	–	Lamarque et al. (2008)
3	CCSRNIES	NIES, Tsukuba, Japan	T42	0.012 hPa	REF	fODS	fGHG	Akiyoshi et al. (2009)
4	CMAM	MSC, University of Toronto, York Univ., Canada	T31	0.00081 hPa	$3 \times$ REF	$3 \times$ fODS	$3 \times$ fGHG	Scinocca et al. (2008); deGrandpre et al. (2000)
5	CNRM-ACM	Meteo-France; France	T63	0.07 hPa	REF	–	–	Déqué (2007); Teysse�re et al. (2007)
6	E39CA	DLR, Germany	T30	10 hPa	REF (with solar cycle & QBO)	–	fGHG	Stenke et al. (2009); Garny et al. (2009)
7	EMAC-FUB	FU Berlin, Germany	T42	0.01 hPa	REF (with solar cycle & QBO)	–	fGHG	J�ckel et al. (2006); Nissen et al. (2007)
8	GEOSCCM	NASA/GSFC, USA	$2^\circ \times 2.5^\circ$	0.015 hPa	REF	fODS	–	Pawson et al. (2008)
9	LMDzrepro	IPSL, France	$2.5^\circ \times 3.75^\circ$	0.07 hPa	REF	fODS	–	Jourdain et al. (2008)
10	MRI	MRI, Japan	T42	0.01 hPa	$2 \times$ REF	fODS	fGHG	Shibata and Deushi (2008a, b)
11	SOCOL	PMOD/WRC and IAC ETHZ, Switzerland	T30	0.01 hPa	$3 \times$ REF	fODS	fGHG	Schraner et al. (2008); Egorova et al. (2005)
12	ULAQ	University of L'Aquila, Italy	$R6/11.5^\circ \times 22.5^\circ$	0.04 hPa	$3 \times$ REF	fODS	fGHG	Pitari et al. (2002); Eyring et al. (2006; 2007)
13	UMSLIMCAT	University of Leeds, UK	$2.5^\circ \times 3.75^\circ$	0.01 hPa	REF	fODS	–	Tian and Chipperfield (2005); Tian et al. (2006)
14	UMUKCA-METO	MetOffice, UK	$2.5^\circ \times 3.75^\circ$	84 km	REF	–	–	Morgenstern et al. (2008, 2009)
15	UMUKCA-UCAM	University of Cambridge, UK and NIWA, NZ	$2.5^\circ \times 3.75^\circ$	84 km	REF	–	–	Morgenstern et al. (2008, 2009)
16	WACCM	NCAR, USA	$1.9^\circ \times 2.5^\circ$	5.9603×10^{-6} hPa	$3 \times$ REF	fODS	fGHG	Garcia et al. (2007)

'Multi-model
assessment of ozone
return dates and
recovery

V. Eyring et al.

Table 2. Specifics of the sensitivity simulations with fixed ODSs (fODS) and fixed GHGs (fGHG). REF1/REF2 are the reference simulations for runs performed under CCMVal-1; REF-B2 the reference simulation for a run performed under CCMVal-2.

CCM		fODS			fGHG				
	Comparison to CCMVal reference run (time period)	Halogens fixed at 1960 levels for chemistry	Halogens fixed at 1960 levels for radiation	SSTs/SICs	Comparison to CCM-Val reference run (time period)	GHGs fixed at 1960 levels for chemistry	GHGs fixed at 1960 levels for radiation	SSTs/SICs	
CCSRNIES	REF (1960–2100)	YES	YES	REF	REF (1960–2100)	YES for CO ₂ , CH ₄ , and N ₂ O	YES for CO ₂ , CH ₄ , and N ₂ O	REF 1955–1964 mean	
CMAM	REF (1960–2100)	YES	NO	Coupled ocean	REF (1960–2100)	NO	YES – including F11, F12	Coupled ocean	
E39CA	–	–	–	–	REF (1960–2050) with natural variability	YES for CO ₂ and CH ₄ , but NO for N ₂ O	YES for CO ₂ , CH ₄ , and N ₂ O	REF 1955–1964 mean	
EMAC-FUB	–	–	–	–	REF (1960–2100) with natural variability	YES for CO ₂ , CH ₄ , and N ₂ O	YES for CO ₂ , CH ₄ , and N ₂ O	REF 1955–1964 mean	
GEOSCCM	REF1 (1960–2004) REF2 (2001–2100)	YES	YES	Hadley Obs/ NCAR CCSM3	–	–	–	–	
LMDZ repro	REF (1960–2100)	YES	YES	Same as REF	–	–	–	–	
MRI	REF (1960–2100)	YES	Radiation does not treat halogens	Same as REF	REF (1960–2100)	YES for CO ₂ , CH ₄ , and N ₂ O	YES for CO ₂ , CH ₄ , and N ₂ O	REF 1955–1964 mean	
SOCOL	REF (1960–2100)	YES	YES	Same as REF	REF (1960–2100)	YES	YES	Same as REF (i.e. not fixed at 1960 conditions)	
ULAQ	REF (1960–2100)	YES	NO	Same as REF	REF (1960–2100)	NO	YES	REF 1955–1964 mean	
UMSLIMCAT	REF (1960–2100)	YES	YES	Same as REF	–	–	–	–	
WACCM	REF (1960–2100)	YES	YES	Same as REF	REF (1960–2100)	YES for CO ₂ , CH ₄ , and N ₂ O	YES for CO ₂ , CH ₄ , and N ₂ O	REF 1955–1964 mean	

Title Page

Abstract

Introduction

Conclusions

References

Tables

Figures

⏪

⏩

◀

▶

Back

Close

Full Screen / Esc

Printer-friendly Version

Interactive Discussion

'Multi-model assessment of ozone return dates and recovery

V. Eyring et al.

Title Page

Abstract

Introduction

Conclusions

References

Tables

Figures

⏪

⏩

◀

▶

Back

Close

Full Screen / Esc

Printer-friendly Version

Interactive Discussion

Table 3. Date of return to 1980 total column ozone in the reference simulations as derived from Fig. 11.

Region	Year of baseline adjustment	Year when MMT ozone returns to 1980 value	Year when lower bound of error bar returns to 1980	Year when upper bound of error bar returns to 1980
Global annual mean	1960	2034	2025	2043
	1980	2034	2028	2040
Tropics annual mean	1960	2052	2028	–
	1980	2049	2034	–
Midlatitude NH annual mean	1960	2021	2014	2030
	1980	2021	2017	2027
Midlatitude SH annual mean	1960	2036	2028	2044
	1980	2037	2031	2043
Antarctic October mean	1960	2052	2045	2062
	1980	2052	2047	2059
Arctic March mean	1960	2026	2020	2035
	1980	2027	2023	2031

'Multi-model assessment of ozone return dates and recovery

V. Eyring et al.

Title Page

Abstract

Introduction

Conclusions

References

Tables

Figures

⏪

⏩

◀

▶

Back

Close

Full Screen / Esc

Printer-friendly Version

Interactive Discussion

Table 4. Summary of the extent to which ozone has returned to 1960 and 1980 levels from its absolute minimum, expressed as percentages calculated from the 1980 baseline-adjusted timeseries of all 16 CCMs' reference simulations. 0% denotes that ozone has not increased above the minimum, 50% denotes that ozone at this date is halfway between the minimum observed and the 1960 or 1980 level, 100% denotes that ozone has returned to the 1960 or 1980 level, and >100% denotes that ozone exceeds the 1960 or 1980 level at this date.

Region	Reference Year; in brackets DU	Year when minimum occurs; in brackets DU	Difference to reference year in 2025	(%)	Difference to reference year in 2050	(%)	Difference to reference year in 2075	(%)	Difference to reference year in 2100	(%)
Unit	(a)	(a)	(DU)	(%)	(DU)	(%)	(DU)	(%)	(DU)	(%)
Global annual mean	1960 (313 DU)	2001 (296 DU)	-8.9	48%	-2.0	89%	1.9	111%	4.3	119%
	1980 (307 DU)		-2.6	76%	4.3	140%	8.2	176%	10.6	188%
Tropics annual mean	1960 (272 DU)	2001 (264 DU)	-4.1	44%	-2.3	70%	-3.0	60%	-7.5	27%
	1980 (270 DU)		-1.9	64%	-0.0	100%	-0.7	87%	-5.3	39%
Midlatitude NH annual mean	1960 (359 DU)	2000 (344 DU)	-3.4	76%	5.3	136%	11.8	179%	21	213%
	1980 (353 DU)		2.3	124%	11.0	220%	15.3	290%	27	344%
Midlatitude SH annual mean	1960 (349 DU)	2002 (321 DU)	-16.3	43%	-3.6	87%	4.7	117%	12.8	130%
	1980 (339 DU)		-5.6	68%	7.0	139%	14.3	186%	23.4	207%
Antarctic October mean	1960 (386 DU)	2003 (245 DU)	-103	25%	-65.0	54%	-36.6	74%	-9.7	93%
	1980 (325 DU)		-43.4	46%	-4.7	94%	23.7	130%	50.6	163%
Arctic March mean	1960 (466 DU)	2002 (425 DU)	-18.8	55%	1.1	103%	17.6	142%	30.4	173%
	1980 (449 DU)		-1.2	95%	18.7	178%	35.2	246%	48.1	300%

'Multi-model assessment of ozone return dates and recovery

V. Eyring et al.

Table 5. Level of confidence that full ozone recovery has already occurred at the end of the century (2090–2097) calculated from the student t-test applied to the multi-model means of the fixed ODS simulation (fODS) and the reference simulation (REF), see text for details. If the confidence level is above 66%, then the year when the confidence level reaches 66% is also added, indicating that full ozone recovery has occurred within 1σ confidence.

Region	Total column ozone	Ozone at 5 hPa	Ozone at 50 hPa
Global annual mean	55%	not assessed here	not assessed here
Tropics annual mean	82% (66% in 2069)	44%	94% (66% in all the years)
Midlatitude NH annual mean	72% (66% in 2072)	26%	89% (66% in 2041)
Midlatitude SH annual mean	61%	28%	83% (65% in 2072)
Arctic March mean	85% (66% in 2036)	not assessed here	91% (66% in 2044)
Antarctic October mean	62%	not assessed here	56%

Title Page

Abstract

Introduction

Conclusions

References

Tables

Figures

⏪

⏩

◀

▶

Back

Close

Full Screen / Esc

Printer-friendly Version

Interactive Discussion

'Multi-model assessment of ozone return dates and recovery

V. Eyring et al.

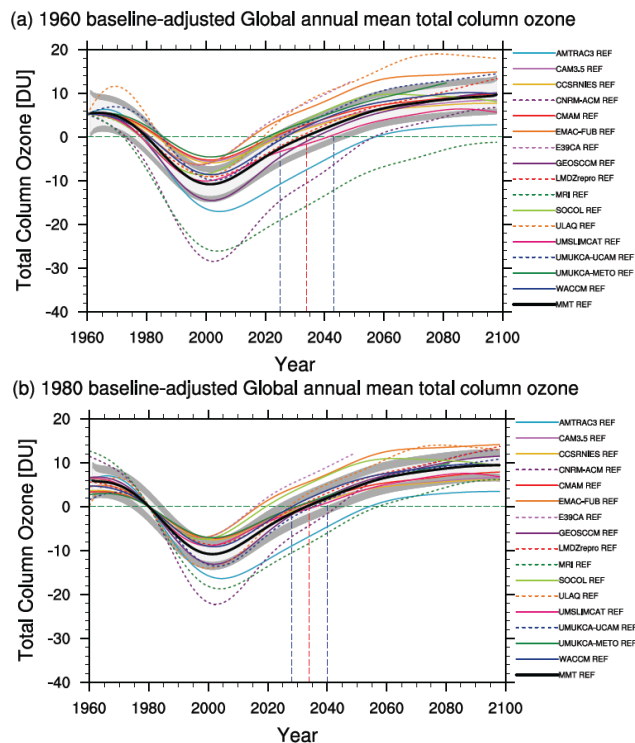


Fig. 1. (a) 1960 and (b) 1980 baseline-adjusted annual mean global total ozone column from the 16 reference simulations (REF). The thick black line shows the multi-model mean and the light- and dark-grey shaded regions show the 95% confidence and 95% prediction intervals, respectively. The red vertical dashed line indicates the year when the multi-model mean returns to 1980 values and the blue vertical dashed lines indicate the uncertainty in these return dates. The uncertainty of ozone returning to 1980 values in the 1960-baseline adjusted time series is larger than in the 1980-baseline adjusted time series (see also Chapter 9 of SPARC CCMVal, 2010).

'Multi-model assessment of ozone return dates and recovery

V. Eyring et al.

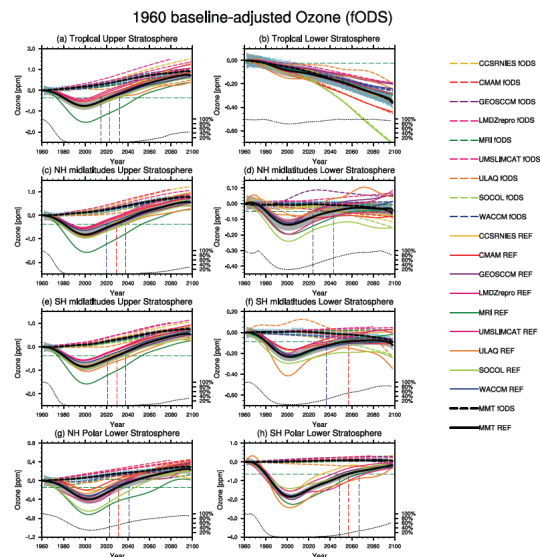


Fig. 2. 1960 baseline-adjusted ozone projections from the reference simulations (REF) compared to the fixed halogen simulations (fODS) for **(a)** 5 hPa and **(b)** 50 hPa tropics annual mean (25° S– 25° N), **(c)** 5 hPa and **(d)** 50 hPa NH midlatitudes annual mean (35° N– 60° N), **(e)** 5 hPa and **(f)** 50 hPa SH midlatitudes annual mean (35° S– 60° S), **(g)** 50 hPa Arctic March mean (60° N– 90° N), and **(h)** 50 hPa Antarctic October mean (60° S– 90° S). The red vertical dashed line indicates the year when the multi-model mean in REF returns to 1980 values and the blue vertical dashed lines indicate the uncertainty in these return dates. The multi-model means calculated from 9 CCMs (CCSRNIES, CMAM, GEOSCCM, LMDZrepro, MRI, SOCOL, UMSLIMCAT, UFAQ, and WACCM) are shown with the black solid (REF) and black dashed line. For clarity, only the 95% confidence intervals are shown (grey and blue shaded area). The dotted black line shows the results of the t-test's confidence level that the multi-model means from fODS and REF are from the same population (see Sect. 5 for details). Note that the y-ranges vary among the panels.

Title Page

Abstract

Introduction

Conclusions

References

Tables

Figures

◀

▶

◀

▶

Back

Close

Full Screen / Esc

Printer-friendly Version

Interactive Discussion

'Multi-model assessment of ozone return dates and recovery

V. Eyring et al.

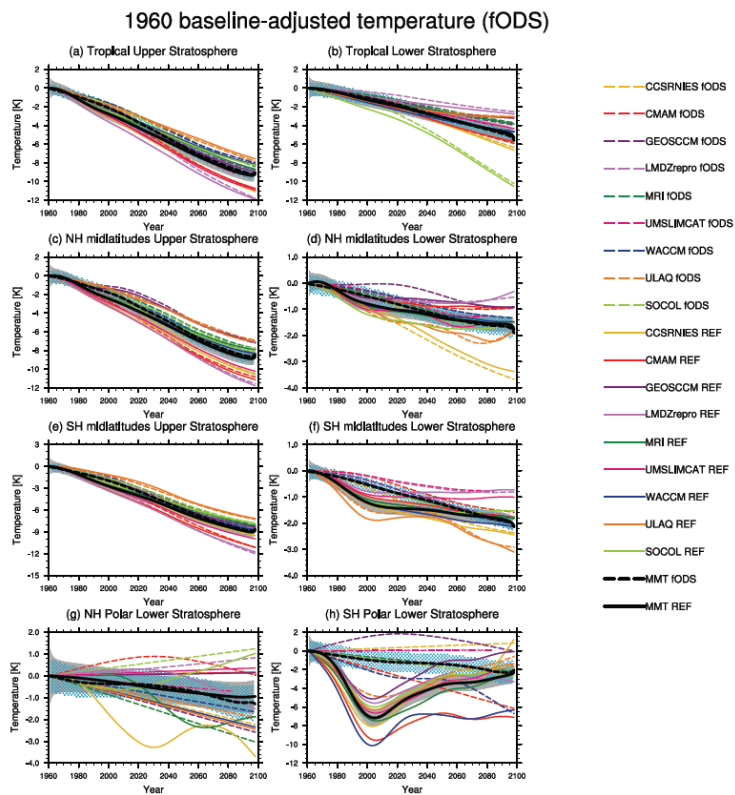


Fig. 3. Same as Fig. 2, but for temperature shown for the reference simulations (REF) and the fixed ODS simulations (fODS). Note that the y-ranges vary among the panels.

Title Page

Abstract

Introduction

Conclusions

References

Tables

Figures

◀

▶

◀

▶

Back

Close

Full Screen / Esc

Printer-friendly Version

Interactive Discussion

**'Multi-model
assessment of ozone
return dates and
recovery**

V. Eyring et al.

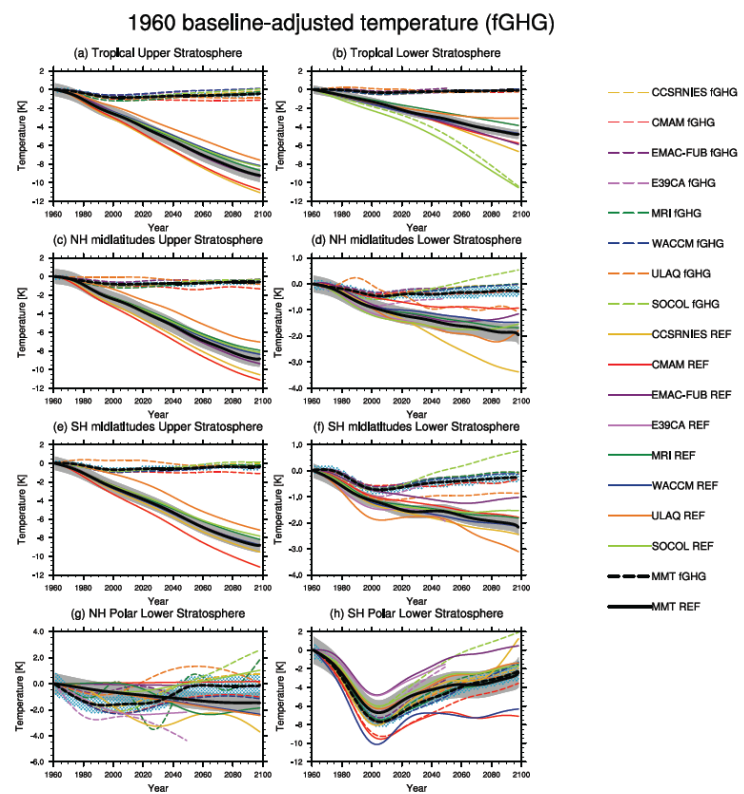


Fig. 4. Same as Fig. 2, but for temperature shown for the reference simulation (REF) and the fixed GHG simulation (fGHG). The multi-model mean is calculated from the 6 CCMs (CCSRNIES, CMAM, E39CA, MRI, ULAQ, and WACCM). SOCOL is not included because of varying SSTs in the fGHG simulation. Note that the y-ranges vary among the panels.

Title Page

Abstract Introduction

Conclusions References

Tables Figures

⏪ ⏩

◀ ▶

Back Close

Full Screen / Esc

Printer-friendly Version

Interactive Discussion



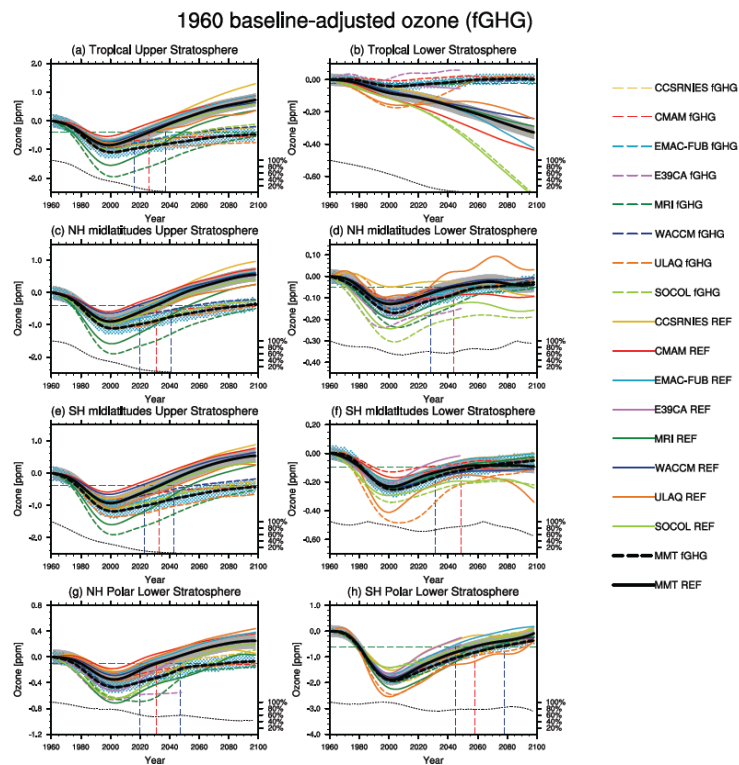


Fig. 5. Same as Fig. 4, but for ozone shown for the reference simulation (REF) and the fixed GHG simulation (fGHG). Note that the y-ranges vary among the panels.

'Multi-model assessment of ozone return dates and recovery

V. Eyring et al.

Title Page

Abstract

Introduction

Conclusions

References

Tables

Figures



Back

Close

Full Screen / Esc

Printer-friendly Version

Interactive Discussion



'Multi-model assessment of ozone return dates and recovery

V. Eyring et al.

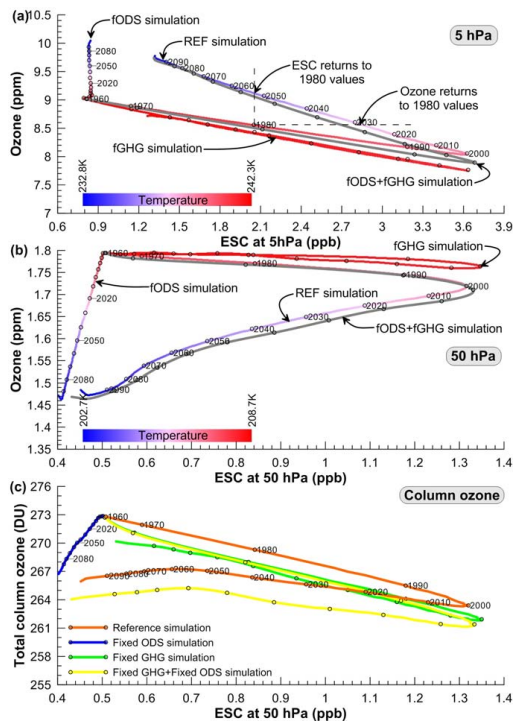


Fig. 6. (a) Annual multi-model mean tropical ozone as a function of $ESC = Cl_y + 5 \times Br_y$ at 5 hPa and averaged between $25^\circ S$ and $25^\circ N$. (b) as in panel (a) but at 50 hPa and where $ESC = Cl_y + 60 \times Br_y$. In panels (a) and (b) the REF, fODS, and fGHG simulations are shown using traces colored according to the multi-model-mean temperature using the scale shown in the bottom left of each panel. The grey traces in these two panels show the additive effects of the fODS and fGHG simulations calculated from: $Grey_{ESC}(t) = fGHG_{ESC}(t) + fODS_{ESC}(t) - fODS_{ESC}(1960)$ and $Grey_{ozone}(t) = fGHG_{ozone}(t) + fODS_{ozone}(t) - fODS_{ozone}(1960)$. Differences between the grey and REF traces indicate a lack of linear additivity in the system. Panel (c), as in (b) but for total column ozone and without color coding by temperature. In this panel the fODS+fGHG trace is shown in yellow (yellow = blue + green). In all three panels, on each trace, reference years are shown every 10th data point with year labels shown for the REF simulation. The multi-model means displayed in this figure were derived from a subset of the 6 models that provided both fGHG and fODS simulations (see text for details).

Title Page

Abstract

Introduction

Conclusions

References

Tables

Figures

◀

▶

◀

▶

Back

Close

Full Screen / Esc

Printer-friendly Version

Interactive Discussion

'Multi-model assessment of ozone return dates and recovery

V. Eyring et al.

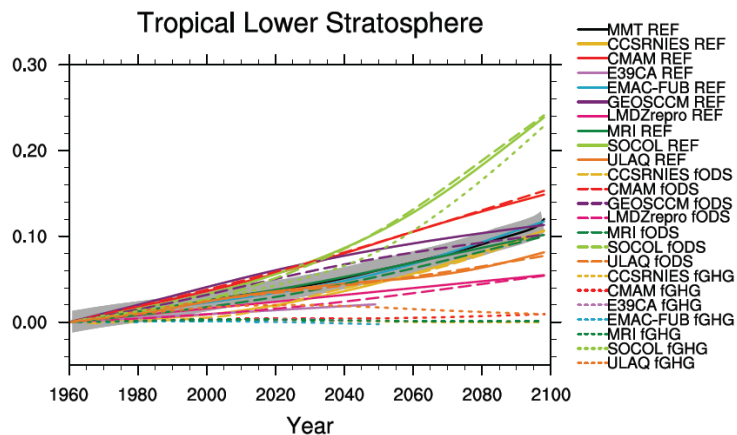


Fig. 7. 1960 baseline-adjusted annual mean w^* between 20°S and 20°N at 70 hPa from the reference simulations (REF) compared to the fixed halogen simulations (fODS) and fixed GHG simulations (fGHG). Shown are the individual models in colors and the MMT of the reference simulations (black line) plus 95% prediction interval (grey shaded area).

Title Page

Abstract

Introduction

Conclusions

References

Tables

Figures

◀

▶

◀

▶

Back

Close

Full Screen / Esc

Printer-friendly Version

Interactive Discussion

'Multi-model assessment of ozone return dates and recovery

V. Eyring et al.

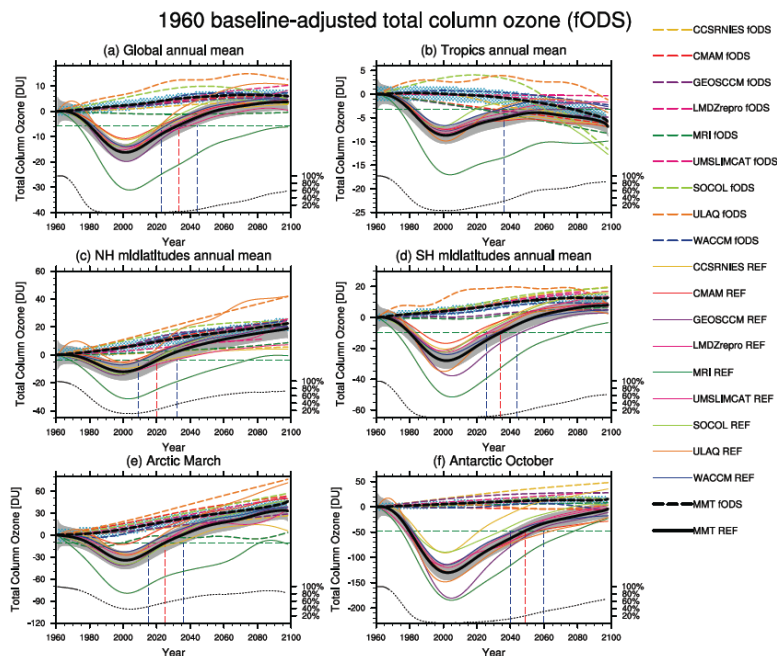


Fig. 8. Same as Fig. 2, but for total column ozone projections in the reference simulations (REF) compared to the fixed halogen simulation (fODS): **(a)** global (90° S– 90° N annual mean), **(b)** in the tropics (25° S– 25° N annual mean), **(c)** NH mid latitudes (35° N– 60° N annual mean), **(d)** SH mid latitudes (35° S– 60° S), **(e)** Arctic (60° N– 90° N March mean), and **(f)** Antarctic (60° S– 90° S October mean). Note that the y-ranges vary among the panels.

Title Page

Abstract

Introduction

Conclusions

References

Tables

Figures



Back

Close

Full Screen / Esc

Printer-friendly Version

Interactive Discussion

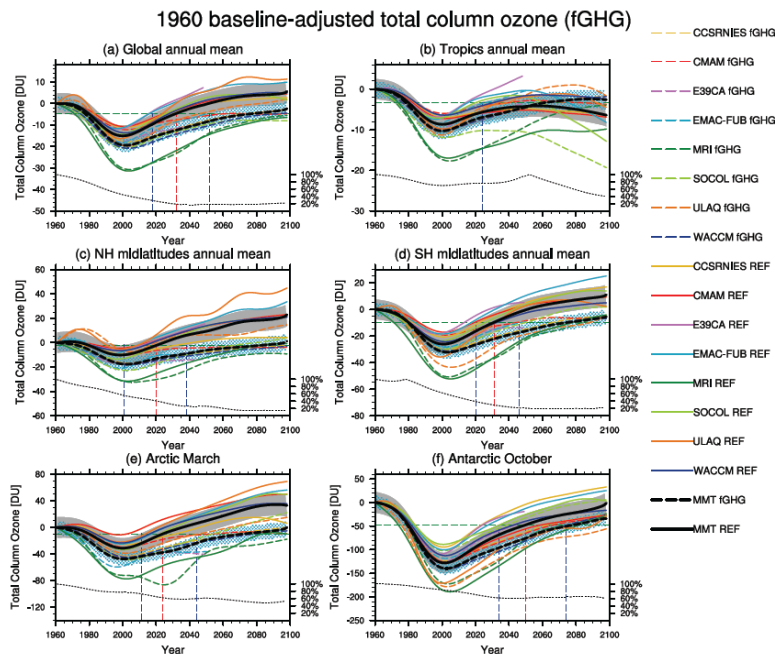


Fig. 9. Same as Fig. 5, but 1960 baseline-adjusted total column ozone projections in the reference simulations (REF) compared to the fixed GHG simulation (fGHG). Note that the y-ranges vary among the panels.

'Multi-model assessment of ozone return dates and recovery

V. Eyring et al.

Title Page

Abstract

Introduction

Conclusions

References

Tables

Figures

◀

▶

◀

▶

Back

Close

Full Screen / Esc

Printer-friendly Version

Interactive Discussion

'Multi-model assessment of ozone return dates and recovery

V. Eyring et al.

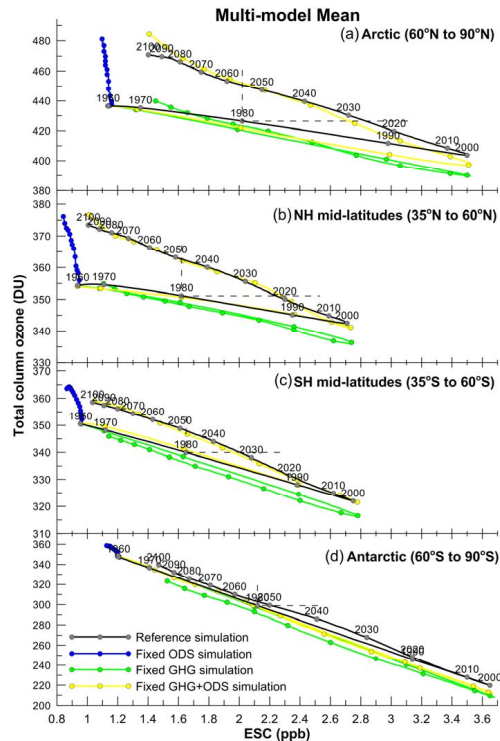


Fig. 10. As in Fig. 6, but for total column ozone in the midlatitudes (annual average) and polar regions (March mean in Arctic and October mean in Antarctic). The multi-model mean is calculated from all models that performed both fODS and fGHG simulations in addition to REF i.e. CCSRNIES, CMAM, MRI, SOCOL, ULAQ and WACCM. ESC is shown for 50 hPa. Blue traces show results from simulations where prescribed ODSs are fixed at 1960 values (fODS). Green traces show results from simulations where prescribed GHGs are fixed at 1960 values (fGHG). Grey traces show the additive effects of the fODS and fGHG simulations calculated from: $Grey_{ESC}(t) = fGHG_{ESC}(t) + fODS_{ESC}(t) - fODS_{ESC}(1960)$ and $Grey_{ozone}(t) = fGHG_{ozone}(t) + fODS_{ozone}(t) - fODS_{ozone}(1960)$. Differences between the grey and REF traces are indicative for a lack of linear additivity in the system.

'Multi-model assessment of ozone return dates and recovery

V. Eyring et al.

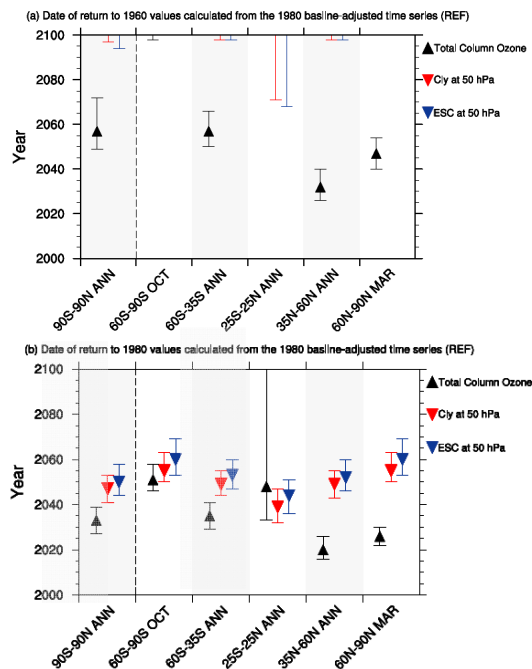


Fig. 11. Date of return to 1960 (upper panel) and 1980 (lower panel) total column ozone (black triangle and error bar), Cl_y at 50 hPa (red triangle and error bar) and ESC at 50 hPa (blue triangle and error bar) for the annual average (global, tropical and midlatitude) and spring (polar) total ozone column derived from the 1980 baseline-adjusted CCMVal-2 reference simulations (16 CCMs) in each latitude band. The error bar shows the uncertainty in return dates as calculated from the 95% confidence interval. ESC is calculated as $Cl_y + 60 \times Br_y$ except for E39CA (see text). While a few models project a return of tropical total column ozone to 1980 levels, most do not with the result that the 95% TSAM confidence interval extends from 2030 to beyond the end of the century which explains the large error bar in the tropical column ozone return dates in the lower panel.

[Title Page](#)
[Abstract](#)
[Introduction](#)
[Conclusions](#)
[References](#)
[Tables](#)
[Figures](#)
[◀](#)
[▶](#)
[◀](#)
[▶](#)
[Back](#)
[Close](#)
[Full Screen / Esc](#)
[Printer-friendly Version](#)
[Interactive Discussion](#)